



Activation energy based extreme value statistics and size effect in brittle and quasibrittle fracture

Zdeněk P. Bažant^{a,*}, Sze-Dai Pang^{b,1}

^a*Civil Engineering and Materials Science, Northwestern University, 2145 Sheridan Road, CEE, Evanston, IL 60208, USA*

^b*Northwestern University, IL 60208, USA*

Received 18 November 2005; accepted 31 May 2006

Abstract

Because the uncertainty in current empirical safety factors for structural strength is far larger than the relative errors of structural analysis, improvements in statistics offer great promise. One improvement, proposed here, is that, for quasibrittle structures of positive geometry, the understrength factors for structural safety cannot be constant but must be increased with structures size. The statistics of safety factors has so far been generally regarded as independent of mechanics, but further progress requires the cumulative distribution function (cdf) to be derived from the mechanics and physics of failure. To predict failure loads of extremely low probability (such as 10^{-6} to 10^{-7}) on which structural design must be based, the cdf of strength of quasibrittle structures of positive geometry is modelled as a chain (or series coupling) of representative volume elements (RVE), each of which is statistically represented by a hierarchical model consisting of bundles (or parallel couplings) of only two long sub-chains, each of them consisting of sub-bundles of two or three long sub-sub-chains of sub-sub-bundles, etc., until the nano-scale of atomic lattice is reached. Based on Maxwell–Boltzmann distribution of thermal energies of atoms, the cdf of strength of a nano-scale connection is deduced from the stress dependence of the interatomic activation energy barriers, and is expressed as a function of absolute temperature T and stress-duration τ (or loading rate $1/\tau$). A salient property of this cdf is a power-law tail of exponent 1. It is shown how the exponent and the length of the power-law tail of cdf of strength is changed by series couplings in chains and by parallel couplings in bundles consisting of elements with either elastic–brittle or elastic–plastic behaviors, bracketing the softening behavior which is more realistic, albeit more difficult to analyze. The power-law tail exponent, which is 1 on the atomistic scale, is raised by the

*Corresponding author. Tel.: +1 847 491 4025; fax: +1 847 491 4011.

E-mail address: z-bazant@northwestern.edu (Z.P. Bažant).

¹Present address: Department of Civil Engineering, National University of Singapore, Singapore.

hierarchical statistical model to an exponent of $m = 10$ to 50, representing the Weibull modulus on the structural scale. Its physical meaning is the minimum number of cuts needed to separate the hierarchical model into two separate parts, which should be equal to the number of dominant cracks needed to break the RVE. Thus, the model indicates the Weibull modulus to be governed by the packing of inhomogeneities within an RVE. On the RVE scale, the model yields a broad core of Gaussian cdf (i.e., error function), onto which a short power-law tail of exponent m is grafted at the failure probability of about 0.0001–0.01. The model predicts how the grafting point moves to higher failure probabilities as structure size increases, and also how the grafted cdf depends on T and τ . The model provides a physical proof that, on a large enough scale (equivalent to at least 500 RVEs), quasibrittle structures must follow Weibull distribution with a zero threshold. The experimental histograms with kinks, which have so far been believed to require the use of a finite threshold, are shown to be fitted much better by the present chain-of-RVEs model. For not too small structures, the model is shown to be essentially a discrete equivalent of the previously developed nonlocal Weibull theory, and to match the Type 1 size effect law previously obtained from this theory by asymptotic matching. The mean stochastic response must agree with the cohesive crack model, crack band model and nonlocal damage models. The chain-of-RVEs model can be verified and calibrated from the mean size effect curve, as well as from the kink locations on experimental strength histograms for sufficiently different specimen sizes.

© 2006 Published by Elsevier Ltd.

Keywords: Random strength; Failure probability; Maxwell–Boltzmann statistics; Safety factors; Nonlocal damage

1. Nature of problem

The type of probability distribution function (pdf) of structural strength has so far been studied separately from the mechanics of structural failure, as if these were independent problems. For quasibrittle structures, however, such a separation is unjustified because the type of pdf depends on structure size and geometry, and does so in a way that can be determined only by cohesive fracture or damage analysis. Structural safety dictates that the design must be based on extremely small failure probability, about 10^{-6} to 10^{-7} (Duckett, 2005; Melchers, 1987; NKB, 1978).

Since part of the uncertainty stems from the randomness of load, which is in structural engineering taken into account by the load factors (Ellingwood et al., 1982; CIRIA, 1977), the knowledge of the far-left tail of pdf of strength need not extend that far. Based on integrating the product of load and strength distributions (Freudenthal et al., 1966; Haldar and Mahadevan, 2000), joint probability computations show that the probability cut-off up to which the pdf tail must be known need not be as small as 10^{-6} – 10^{-7} , but must still be only about one order of magnitude larger, i.e., about 10^{-5} – 10^{-6} (Bažant, 2004a), provided that, as usual, the load and resistance factors do not differ by more than about 3:1 (this requirement is more stringent if the structural strength distribution has a Weibull, rather than Gaussian, tail).

In the far-left tail, the pdf type makes a huge difference. For example, the difference of load with failure probability 10^{-6} from the mean failure load will almost double when the pdf changes from Gaussian to Weibull (with the same mean and same coefficient of variation (CoV); see Fig. 1).

The importance of the problem is clear from the large values of safety factors. Defined as the ratio of mean load capacity to the maximum service load, they are about 2 in the case

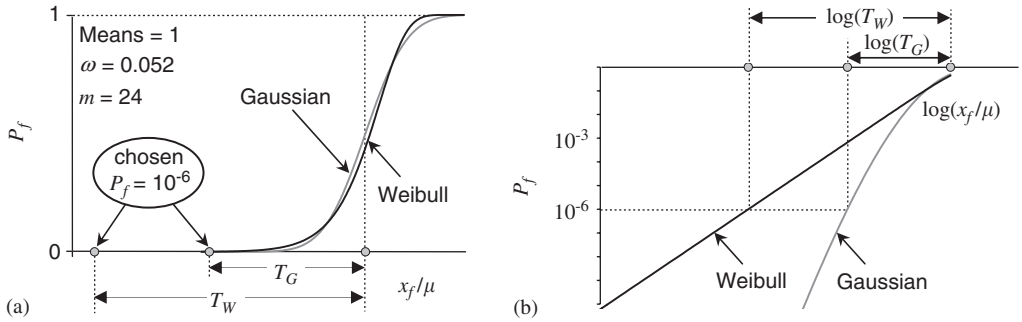


Fig. 1. Large difference between points of failure probability 10^{-6} for Gaussian and Weibull distributions with mean 1 and CoV = 5.2% in (a) linear scale; (b) log scale.

of steel structures, or aeronautical and naval structures, while in the case of brittle failures (e.g., shear failures) of normal size concrete structures they are about 4 for design code formulas and about 3 for finite element simulations (Bažant and Yu, 2006). Consequently, improvements in the stochastic fracture mechanics underlying the safety factors have the potential of bringing about much greater benefits than improvements in the methods of deterministic structural analysis. It makes no sense at all to strive for a 5% to 10% accuracy improvement by more sophisticated computer simulations or analytical solutions and then scale down the resulting load capacity by an empirical safety factor of 2 to 4 which easily could have an error over 50%.

2. Background and objectives

While the mean statistical size effect in failures at macrocrack initiation is by now understood quite well (e.g., Bažant and Planas, 1998, Chapter 12), and its combination with the deterministic size effect has recently also been clarified (Bažant and Xi, 1991; Bažant and Novák, 2000a, b, 2001; Bažant, 2004a, b; Carmeliet, 1994; Carmeliet and Hens, 1994; Gutiérrez, 1999; Breyse, 1990; Frantziskonis, 1998), little is known about the type of pdf to be assumed once the mean structural response has been calculated. What is clear is that the strength of brittle structures made, e.g., of fine-grained ceramics and fatigue-embrittled steel, must follow the Weibull distribution—by virtue of the weakest-link (or series coupling) model (because one small material element will trigger failure), and that (except in the far-out tails) the strength of ductile (or plastic) structures must follow the Gaussian distribution—by virtue of the central limit theorem (CLT) of the theory of probability (because the limit load is a sum of contributions from all the plasticized material elements along the failure surface, as in parallel coupling).

Statistical models with parallel and series couplings have been extensively analyzed, e.g., by Phoenix (1978, 1983), Phoenix and Smith (1983), McCartney and Smith (1983), McMeeking and Hbaieb (1999), Phoenix et al. (1997), Phoenix and Beyerlein (2000), Harlow and Phoenix (1978a, b), Harlow et al. (1983), Rao et al. (1999), Mahesh et al. (2002), Smith (1982) and Smith and Phoenix (1981). However, what seems to have been unappreciated and has been brought to light only recently (Bažant, 2004a, b), on the basis of nonlocal Weibull theory (Bažant and Xi, 1991), is that the pdf of strength of a quasibrittle structure must gradually change with increasing size and shape (or brittleness)

from Gaussian to Weibull (Bažant, 2004a). Consequently, the size effect impacts not only the mean structural strength but also the type of distribution, and thus the understrength part of safety factor.

It might seem that any consideration of failure probabilities as small as 10^{-6} or 10^{-5} would be purely speculative because direct determination of failure load histogram in that probability range would require at least 10^8 tests of identical laboratory specimens. However, there are plenty of physical theories that cannot be directly verified by experiments but are well established because they have been experimentally verified through their predictions. The most important prediction from the tail pdf of material strength is the mean statistical size effect. This can be observed experimentally even though it depends only on the far-left tail of pdf. When structural failure is caused by only one representative volume element (RVE) of the material, a structure consisting of 100^3 RVEs in fact samples the far-left tail of material strength pdf in the 10^{-6} probability range. Another feasible way of verification, of course, is to conduct computer simulations based on a more fundamental theory, for example, the random lattice model (Cusatis et al., 2003).

This article (which expands a recent conference presentation, Bažant and Pang, 2005b, and is briefly summarized, without derivations, in Bažant and Pang, 2006) has three goals: (i) to present a rational physical argument for the evolution of pdf of strength with the size of quasibrittle structures; (ii) to deduce the pdf of strength of the RVE from the statistics of interatomic bond breaks; and (iii) to relate the pdf to activation energy, temperature, load duration and material characteristic length l_0 . At a recent conference (Bažant and Pang, 2005a), the implications for structural reliability analysis, and particularly for generalizing the Cornell (1969) and Hasofer-Lind (Madsen et al., 1986) reliability indices to incorporate the size and shape dependence, have been pointed out.

3. Quasibrittle behavior and size effect

The tail probabilities and the associated size effect have doubtless played a significant role in many disasters of very large civil engineering structures. These disasters have been at least three orders of magnitude more frequent than the failures of small structures (Duckett, 2005; Melchers, 1987; NKB, 1978), and about 10-times more frequent than estimated by recent state-of-art analysis. Reanalysis of the 1959 failure of Malpasset Dam (Bažant et al. 2005b) revealed that if this dam were designed today, with the knowledge of the statistical-energetic size effect on mean structural strength and of the change of pdf from Gaussian to Weibull to be analyzed here, the tolerable displacement of the abutment (which is what doomed this record-breaking structure) would have been about 4-times smaller than what was considered safe in 1950 when this ill-fated dam was designed.

The effect of size (and brittleness) on reliability of quasibrittle structures was clarified by numerical simulations (Bažant and Novák, 2000a, b) and asymptotic approximations (Bažant, 1997, 2004a, b) based on the nonlocal generalization of Weibull theory (Bažant and Xi, 1991)—a theory that can capture both the energetic (deterministic) and statistical size effects (see the reviews in Bažant, 2002, 2004a, b; Bažant and Planas, 1998). For not too small failure probabilities ($P_f \geq 0.05$), Monte Carlo simulations with this theory have been shown to fit well the histograms of extensive tests of flexural strength (modulus of rupture) of concrete (Koide et al., 1998, 2000). An asymptotic-matching formula for the

combined statistical-energetic size effect was shown to match well Jackson's (1992) flexural strength tests of laminates at NASA.

Quasibrittle structures, consisting of quasibrittle materials, are those in which the fracture process zone (FPZ) is not negligible compared to the cross section dimension D (and may even encompass the entire cross section). Depending on the scale of observation or application, quasibrittle materials include concrete, fiber composites, toughened ceramics, rigid foams, nanocomposites, sea ice, consolidated snow, rocks, mortar, masonry, fiber-reinforced concretes, stiff clays, silts, grouted soils, cemented sands, wood, paper, particle board, filled elastomers, various refractories, coal, dental cements, bone, cartilage, biological shells, cast iron, grafoil, and modern tough alloys. In these materials, the FPZ undergoes softening damage, such as microcracking, which occupies almost the entire nonlinear zone. By contrast, in ductile fracture of metals, the FPZ is essentially a point within a nonnegligible (but still small) nonlinear zone undergoing plastic yielding rather than damage.

The width of FPZ is typically about the triple of the dominant inhomogeneity size. Its length can vary enormously; it is typically about 50 cm in normal concretes; 5 cm in high-strength concretes; 10–100 μm in fine-grained ceramics; 10 nm in a silicon wafer; 100 m in a mountain mass intersected by rock joints; 1–10 m in an Arctic sea ice floe; and about 50 km in the ice cover of Arctic Ocean (consisting of thick floes a few km in size, connected by thin ice). If the cross section dimension (size) of structures is far larger than the FPZ size, a quasibrittle material becomes perfectly brittle, i.e., follows linear elastic fracture mechanics (LEFM). Thus, concrete is quasibrittle on the scale of normal beams and columns, but perfectly brittle on the scale of a large dam. Arctic Ocean cover, fine-grained ceramic or nanocomposite are quasibrittle on the scales of 10 km, 0.1 mm or 0.1 μm , but brittle on the scales of 1000 km, 1 cm or 10 μm , respectively.

The FPZ width may be regarded as the size of the RVE of the material. The RVE definition cannot be the same as in the homogenization theory of elastic structures. The RVE is here defined as the smallest material element whose failure causes the failure of the whole structure (of positive geometry). From experience with microstructural simulation and testing, the size of RVE is roughly the triple of maximum inhomogeneity size (e.g., the maximum aggregate size in concrete or grain size in a ceramic).

According to the deterministic theories of elasticity and plasticity, geometrically similar structures exhibit no size effect, i.e., their nominal strength, defined as

$$\sigma_N = P_{\max}/bD \quad (1)$$

is independent of characteristic structure size D (P_{\max} = maximum load of the structure or parameter of load system; b = structure thickness in the third dimension). The size effect is defined as the dependence of σ_N on D . Structures whose material failure criterion is deterministic and involves only the stress and strain tensors exhibit no size effect. The classical cause of size effect, proposed by Mariotte around 1650 and mathematically described by Weibull (1939), is the randomness of strength of a brittle material. Quasibrittle structures, whose material failure criterion involves a material characteristic length l_0 (implied by the material fracture energy or the crack softening curve), exhibit, in addition, the energetic size effect (Bažant, 1984, 2002). This size effect is caused by energy release due to stress redistribution engendered by a large FPZ (or by stable growth of large crack before reaching the maximum load).

Two basic types of energetic size effect must be distinguished. The Type 1 size effect, the only one studied here, occurs in positive geometry structures failing at macrocrack initiation (positive geometry means that the stress intensity factor at constant load increases with the crack length). Type 2 occurs in structures containing a large notch or a large stress-free (fatigued) crack formed prior to maximum load (there also exists a Type 3 size effect, but it is very similar to Type 2); Bažant, 2002. For Type 2, material randomness affects significantly only the scatter of σ_N but not its mean (Bažant and Xi, 1991), while for Type 1 it affects both, and so is more important. Type 1 is typical of flexural failures, in which the RVE size coincides with the thickness of the boundary layer of cracking. This layer causes stress redistribution and energy release before the maximum load is reached. This, in turn, engenders the Type 1 energetic size effect which dwarfs the statistical Weibull-type size effect when the structure is small. A statistical size effect on mean σ_N is significant only for Type 1.

4. Hypotheses of analysis

Hypothesis I. The failure of interatomic bonds is governed by the Maxwell–Boltzmann distribution of thermal energies of atoms and the stress dependence of the activation energy barriers of the interatomic potential.

Hypothesis II. Quasibrittle structures (of positive geometry) that are at least 1000-times larger than the material inhomogeneities, as well as laboratory specimens of sufficiently fine-grained brittle materials, exhibit random strength that follows the Weibull distribution.

Hypothesis III. The cumulative distribution function (cdf) of strength of an RVE of brittle or quasibrittle material may be described as Gaussian (or normal) except in the far-left power-law tail that reaches up to the failure probability of about 0.0001–0.01 (this hypothesis is justified, e.g., by Weibull’s tests of strength histograms of mortar discussed after Eq. (69)).

5. Fundamental questions to answer

In the weakest-link statistical theory of strength, there remain four unanswered fundamental questions:

- (1) What is the physical reason for the tail of the pdf of strength to be a power law?
- (2) Why must the threshold of power-law tail be zero?
- (3) What is the physical meaning of Weibull modulus m ?
- (4) Why is the power law exponent so high, generally 10–50?

A physical justification of Weibull distribution of structural strength was proposed by Freudenthal (1968), who assumed inverse proportionality for the distribution of material flaw sizes, neglecting flaw interactions and material heterogeneity. However, this did not amount to a physical proof because his assumptions were themselves simplifications subjected to equal doubt. Besides, for some quasibrittle materials such as Portland cement concretes, the relevant distribution of material flaws is hardly quantifiable, because the microstructure is totally disordered and saturated with flaws all the way down to

nanometers. As will be shown here, the physical proof can be based on Hypothesis I, which is exposed to no doubt.

6. Strength distribution ensuing from stress dependence of activation energy barriers and Maxwell–Boltzmann distribution

The basic idea, stated in Hypothesis I, is that the failure probability must, in some way, be controlled by interatomic bond breaks. The fraction of atoms (or frequency) at which the thermal energy of an atom at absolute temperature T exceeds \mathcal{E} is known to be given by the Maxwell–Boltzmann distribution: $\Phi(\mathcal{E}) = e^{-\mathcal{E}/kT}$ (e.g., Hill, 1960; Mayer, 1940; Cottrell, 1964; McClintock and Argon, 1966); k = Boltzmann constant. The cdf of \mathcal{E} is then $1 - e^{-\mathcal{E}/kT}$, and the corresponding pdf is $\phi(\mathcal{E}) = e^{-\mathcal{E}/kT}/kT$. If the energy of an atom exceeds its activation energy Q (Fig. 2), its bond gets broken. The frequency, or rate, of interatomic bond breaks is $f_0 = \int_Q^\infty e^{-\mathcal{E}/kT} d\mathcal{E}/kT$ or

$$f_0 = e^{-Q/kT} \tag{2}$$

(which is also known as the Arrhenius equation). Aside from phenomena such as melting, evaporation, desorption, diffusion, chemical reactions, creep and dislocations, bond breaks are what causes fracture.

Because stress is the gradient of potential energy, a macrocontinuum applied stress, σ , causes the activation energy barrier to change from Q to $Q - \kappa\sigma$ for bond breaking (in the sense of stress), and from Q to $Q + \kappa\sigma$ for bond restoration (in the sense opposite to stress); Fig. 2; κ is a positive constant depending on the type and geometry of atomic lattice (this is an argument introduced for viscous flow and diffusion by Eyring, 1934; see also Eyring et al., 1980 and Glasstone et al., 1941). So, the frequency of interatomic bond breaks becomes $e^{-(Q-\kappa\sigma)/kT}$, and the frequency of interatomic bond restorations becomes $e^{-(Q+\kappa\sigma)/kT}$. Hence, the net frequency, f_b , of permanent bond breaks under stress σ at temperature T is $e^{-(Q-\kappa\sigma)/kT} - e^{-(Q+\kappa\sigma)/kT}$, which may be rewritten as

$$f_b = 2e^{-Q/kT} \sinh(\kappa\sigma/kT). \tag{3}$$

It might be objected that this equation does not take into account the transfer of load from broken to unbroken interatomic bonds and the gradual exhaustion of interatomic bonds carrying the applied macroscopic stress σ . However, this load transfer will be captured separately by parallel couplings in the statistical strength model connecting the nano- and macroscales.

A continuous crack within an RVE will occur when the broken bonds create a contiguous surface of atomic bond breaks separating the atomic lattice into two parts. This

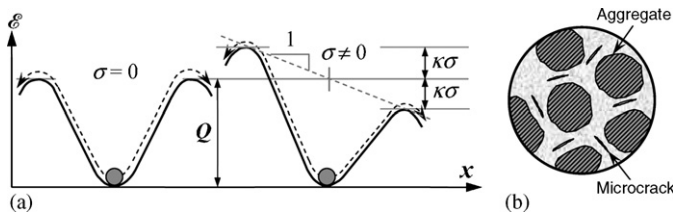


Fig. 2. (a) Interatomic potential profile and change of activation energy caused by applied stress σ ; (b) breaks within matrix connections between inclusions (their number is governed by inclusion packing).

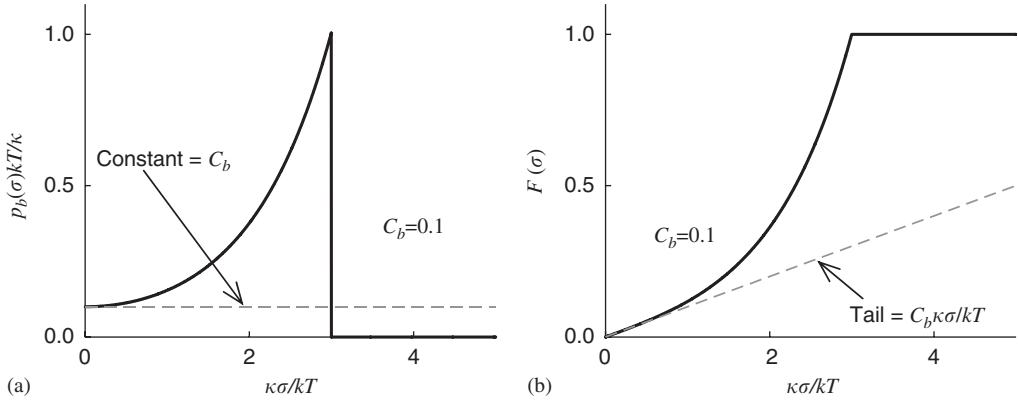


Fig. 3. Effect of applied stress and temperature on the failure probability of interatomic bonds (a) pdf; (b) cdf.

will occur when the fraction of broken bonds in the lattice reaches a certain critical value ϕ_b (the calculation of which is a problem of percolation theory, different from the classical problem of continuous passage channel through the solid). That critical value will be attained after a certain critical duration τ of exposure of the RVE to stress σ , and so $\phi_b = \phi_b(\tau)$. As a crude approximation, one may assume proportionality, i.e., $\phi_b(\tau) \approx \phi_0 \tau$ where ϕ_0 is a constant depending on the type and geometry of the atomic lattice. So, the cumulative probability of creating a continuous crack on the nano-scale may be expressed as

$$F(\sigma) = \min[C_b \sinh(\kappa\sigma/kT), 1] \quad \text{for } \sigma \geq 0, \tag{4}$$

where

$$C_b = 2\phi_b(\tau)e^{-Q/kT}. \tag{5}$$

The “min” serves here to ensure that $F(\sigma)$ terminate at 1. The stress at which $F(\sigma) = 1$ is $\sigma_1 = (kT/\kappa)\sinh^{-1}(1/C_b)$, which is a function of temperature T as well as the stress-duration, τ (thus the time or rate dependence of strength is included in the formulation). The corresponding pdf is (Fig. 3): $p_b = (C_b\kappa/kT) \cosh(\kappa\sigma/kT)$ for $\sigma \in (0, \sigma_1)$; else $p_b = 0$. Of main interest here is the left tail of $F(\sigma)$. Since $\sinh x \approx x$ for small x , the cdf tail is

$$\text{for } \sigma \rightarrow 0 : F(\sigma) \approx (C_b\kappa/kT)\sigma \propto \sigma^p \quad \text{with } p = 1. \tag{6}$$

The important point to note is that the tail is a power law with zero threshold and exponent 1 (thus, for example, the strength of a chain, or a series coupling, of many potential break surfaces on the nano-scale would have a Weibull cdf with $m = 1$, which is the exponential distribution, i.e., $F(\sigma) = 1 - e^{-c\sigma}$ in which $c = C_b\kappa/kT$; however, the exponential distribution is not needed for our purpose and probably would anyway be an oversimplification, because the break surfaces do not interact as simply as the links in a chain).

6.1. Review of Weibull weakest-link model and its nonlocal generalization

To make the statistical connection from the nano-scale of atoms to the macroscale of the FPZ or the structure, various probabilistic models of strength need to be discussed. First

we discuss the simplest, which is the weakest-link model (Fig. 4(a)). This model is applicable if the FPZ is so small in comparison to structure size D that it can be treated as a point. For geometrically similar structures of various sizes, the stress distribution as a function of relative coordinate vector $\xi = \mathbf{x}/D$ of material points is then independent of D (\mathbf{x} = actual coordinate vector). The structure may be considered as an assembly of small material elements, the size of which is the same as the size of the laboratory test specimens. Conveniently (but not necessarily, for the purpose of statistics alone), these material elements will be assumed to coincide with the RVE, whose volume is V_0 and size is $l_0 = V_0^{1/n_d}$ = material characteristic length.

Denote P_k = failure probability of the k th RVE ($k = 1, 2, \dots, N$) of structure, and P_f = failure probability of the structure. In structures of positive geometry, to which this study is restricted, the failure of one RVE causes the whole structure to fail. Then the probability of survival of the structure is the joint probability of survival of all the RVEs. Assuming

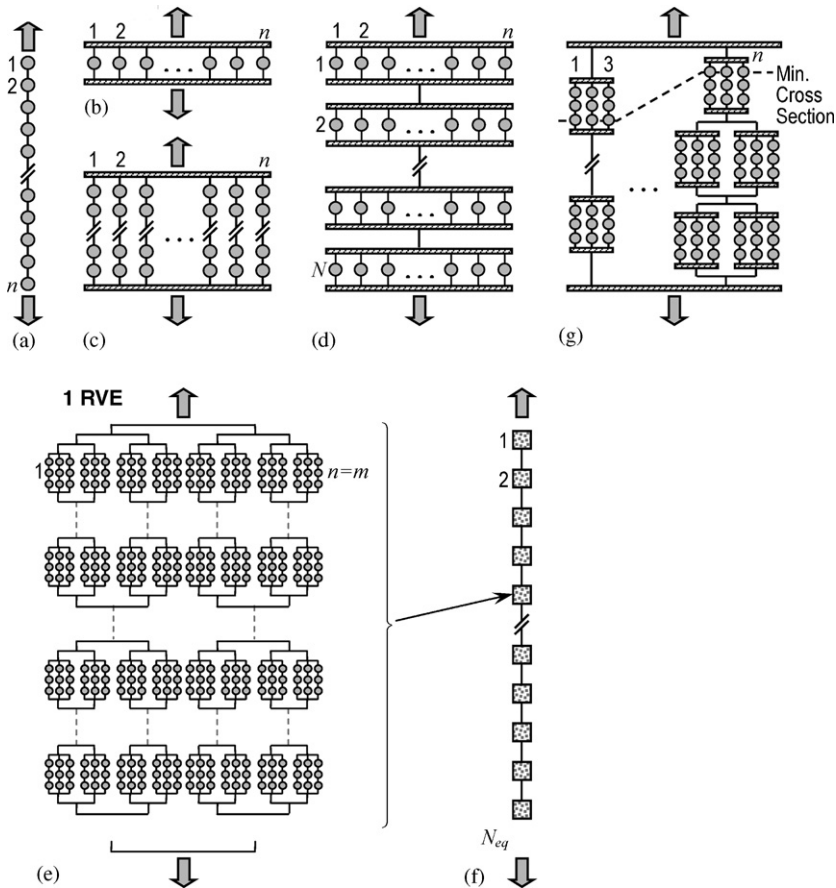


Fig. 4. Models of series and parallel couplings of brittle elements (chains of links and fiber bundles): (a) chain; (b) fiber bundle; (c) bundle of chains; (d) chain of bundles; (e) a feasible idealized model, involving a hierarchy of sub-chains and sub-bundles; (f) a weakest-link model made up of elements, each representing one RVE by the hierarchical model in (e); and (g) example of a complex irregular hierarchical model with sub-chains and sub-bundles.

that all P_k are statistically uncorrelated, we thus have $1 - P_f = (1 - P_1)(1 - P_2) \cdots (1 - P_N)$, or

$$\ln(1 - P_f) = \sum_{k=1}^N \ln(1 - P_k) \approx - \sum_{k=1}^N P_k, \quad (7)$$

where we set $\ln(1 - P_k) \approx -P_k$ because a long chain must fail as $P_k \ll 1$. Based on experiments, Weibull (1939, 1951) realized that, to fit test data, the left (low probability) tail of the cdf of RVE strength (i.e., failure probability of one RVE) must be a power law, i.e.,

$$P_k = [\sigma(\mathbf{x}_k)/s_0]^m \quad \text{for small } \sigma(\mathbf{x}_k), \quad (8)$$

where s_0 and m are material constants called the scale parameter and Weibull modulus (or shape parameter); and $\sigma(\mathbf{x}_k)$ is the positive part of the maximum principal stress at a point of coordinate vector \mathbf{x}_k (the positive part is taken because negative normal stresses do not cause tensile fracture). Substituting this into (7) and making a limit transition from discrete sum to an integral over structure volume V , one gets the well-known Weibull probability integral:

$$- \ln(1 - P_f) = \sum_k \left(\frac{\sigma(\mathbf{x}_k)}{s_0} \right)^m \approx \int_V \left(\frac{\sigma(\mathbf{x})}{s_0} \right)^m \frac{dV(\mathbf{x})}{l_0^{n_d}}. \quad (9)$$

The integrand $[\sigma(\mathbf{x}_k)/s_0]^m/l_0^{n_d} = c_f(\mathbf{x})$ is called the spatial concentration of failure probability and is the continuum equivalent of P_k per volume $l_0^{n_d}$. Because the structure strength depends on the minimum strength value in the structure, which is always small if the structure is large, the validity of Eq. (9) for large enough structures is unlimited.

Consider now geometrically similar structures of different sizes D in which the dimensionless stress fields $\bar{\sigma}(\xi)$ are the same functions of dimensionless coordinate vector $\xi = \mathbf{x}/D$, i.e., depend only on structure geometry but not on structure size D . In Eq. (9), we may then substitute $\sigma(\mathbf{x}) = \sigma_N \bar{\sigma}(\xi)$ where $\sigma_N =$ nominal stress $= P/bD$; $P =$ applied load or a conveniently defined load parameter, and $b =$ structure width (which may but need not be scaled with D). Further we may set $dV(\mathbf{x}) = D^{n_d} dV(\xi)$ where $n_d =$ number of spatial dimensions in which the structure is scaled ($n_d = 1, 2$ or 3). After rearrangements, Eq. (9) yields $-\ln(1 - P_f) = (\sigma_N/S_0)^m$, or

$$P_f = 1 - e^{-(\sigma_N/s_0)^m \Psi(D/l_0)^{n_d}} = 1 - e^{-(\sigma_N/S_0)^m}, \quad (10)$$

where

$$S_0 = s_0(l_0/D)^{n_d/m} \Psi^{-1/m}, \quad \Psi = \int_V [\bar{\sigma}(\xi)]^m dV(\xi). \quad (11)$$

According to Eq. (10), the tail probability is a power law:

$$P_f \approx (\sigma_N/S_0)^m \quad (\text{for } \sigma_N \rightarrow 0). \quad (12)$$

For $P_f \leq 0.02$ (or 0.2), its deviation from Eq. (10) is $< 1\%$ (or $< 10\%$) of P_f .

The effect of structure geometry is embedded in integral Ψ , independent of structure size. Because exponent m in this integral is typically around 25, the regions of structure in which the stress is less than about 80% of mean material strength have a negligible effect.

Note that P_f depends only on the parameter

$$s_0^* = s_0 l_0^{n_d/m} \quad (13)$$

and not on s_0 and l_0 separately. So, the material characteristic length l_0 is used here only for convenience, to serve as a chosen unit of measurement. The Weibull statistical theory of strength, per se, has no characteristic length (which is manifested by the fact that the scaling law for the mean strength is a power law; Bažant, 2002). However, in the generalization to the probabilistic-energetic theory of failure and size effect (Eq. (25)), the use of material characteristic length is essential, which is why introducing l_0 is here convenient.

The last expression in Eq. (10) is the Weibull cdf in standard form, with scale parameter S_0 . From Eq. (11) one finds that

$$\sigma_N = C_0 (l_0/D)^{n_d/m}, \quad (14)$$

where

$$C_0 = C_f \Psi^{-1/m}, \quad C_f = s_0 [-\ln(1 - P_f)]^{1/m}. \quad (15)$$

This equation, in which C_0 and S_0 are independent of D , describes the scaling of nominal strength of structure for a given failure probability P_f . The mean nominal strength is calculated as $\bar{\sigma}_N = \int_0^\infty \sigma_N p_f(\sigma_N) d\sigma_N$ where $p_f(\sigma_N) = dP_f(\sigma_N)/d\sigma_N = \text{pdf}$ of structural strength. Substituting Eq. (10), one gets, after rearrangements, the well-known Weibull scaling law for the mean nominal strength as a function of structure size D and geometry parameter Ψ ;

$$\bar{\sigma}_N(D, \Psi) = s_0 \Gamma(1 + 1/m) = C_s(\Psi) D^{-n_d/m}, \quad (16)$$

where

$$C_s(\Psi) = \Gamma(1 + 1/m) l_0^{n_d/m} s_0 / \Psi^{1/m} \quad (17)$$

in which one may use the approximation $\Gamma(1 + 1/m) \approx 0.6366^{1/m}$ for $5 \leq m \leq 50$ (Bažant and Planas, 1998, Eq. 12.1.22).

The CoV of σ_N is calculated as $\omega_N^2 = [\int_0^\infty \sigma_N^2 dP_f(\sigma_N)] / \bar{\sigma}_N^2 - 1$. Substitution of Eq. (10) gives, after rearrangements, the following well-known expression:

$$\omega_N = \sqrt{\frac{\Gamma(1 + 2/m)}{\Gamma^2(1 + 1/m)} - 1} \quad (18)$$

which is independent of structure size as well as geometry. Approximately, $\omega_N \approx (0.462 + 0.783m)^{-1}$ for $5 \leq m \leq 50$ (Bažant and Planas, 1998, Eq. 12.1.28).

It is conceptually useful to introduce the equivalent number, N_{eq} , of RVEs for which a chain with N_{eq} links gives the same cdf. For a chain under the same tensile stress $\sigma = \sigma_N$ in each element, we have

$$P_f = 1 - e^{-N_{\text{eq}}(\sigma_N/s_0)^m}. \quad (19)$$

Setting this equal to (10) and solving for N , we obtain

$$N_{\text{eq}} = (s_0/S_0)^m = (D/l_0)^{n_d} \Psi. \quad (20)$$

N_{eq} is here a more convenient alternative to what is called the Weibull stress (Beremin, 1983), σ_W , which is defined by setting

$$P_f = 1 - e^{-(\sigma_W/s_0)^m} = 1 - e^{-(V_{\text{eff}}/V_0)(\sigma_N/s_0)^m}, \quad (21)$$

where $V_{\text{eff}}/V_0 = (D/l_0)^{n_d} \Psi$. Equating this to (10), we see that

$$\sigma_W = \sigma_N \Psi^{1/m} (D/l_0)^{n_d/m} = \sigma_N N_{\text{eq}}^{1/m} \quad (22)$$

i.e., the Weibull stress is the nominal stress corrected for the size and geometry factors.

Eq. (21) is a popular way to express the statistical size effect V as a ‘volume effect’. But this term may be misleading. In Eqs. (9) and (11) the integration over V of a three-dimensional structure must be made two-dimensionally ($n_d = 2$) if the structure must fail, for reasons of mechanics, simultaneously through its entire width b (i.e., the initiating fracture front is not a short segment within the beam width but a line through the entire width). Otherwise, widening a narrow beam, which increases the structure volume V , would be predicted to reduce the strength of the beam, but this would contradict experience. For this reason, calling the statistical size effect the volume effect is not quite accurate.

Eq. (10) can alternatively be deduced from the stability postulate of extreme value statistics, expressed by the following functional equation for survival probability $\Phi(\sigma)$ (Fréchet, 1927);

$$\Phi^N(\sigma) = \Phi(a_N \sigma + b_N), \quad \Phi(\sigma) = 1 - P_f(\sigma). \quad (23)$$

To derive it, one imagines the chain to be subdivided into N sub-chains, each with survival probability $\Phi(\sigma)$. Because the chain survives only if all sub-chains survive, the survival probability of the chain must be the joint probability of survival of all sub-chains, which is $\Phi^N(\sigma)$. The survival probability $\Phi(\sigma)$ of each sub-chain must obviously be similar, i.e., related to $\Phi^N(\sigma)$ by linear transformation, characterized in Eq. (23) by coefficients a_N and b_N . Substitution of Eq. (10) verifies that Eq. (23) is indeed satisfied, and that $a_N = N^{1/m}$ and $b_N = 0$.

The domain of attraction of Weibull distribution includes all elemental distributions $P_1(\sigma_1)$ which asymptotically approach a power law. This is mathematically expressed by the condition $\lim_{\sigma_1 \rightarrow 0} [\sigma_1/P_1(\sigma_1)] dP_1(\sigma_1)/d\sigma_1 = m = \text{a positive constant}$ (e.g., Gumbel, 1958; Ang and Tang, 1984). Eq. (10) is such a distribution because, for small σ^m , $1 - e^{-\sigma^m} \approx \sigma^m$, i.e., the Weibull cdf (as well as pdf) has a power-law left tail.

Fisher and Tippett (1928) proved that Eq. (23) can be satisfied by three and only three distributions. Aside from Eq. (10), they are $P_f(\sigma) = 1 - e^{-e^{\sigma/s_N}}$ for $\sigma \in (-\infty, \infty)$, which later came to be known as the Gumbel (1958) (minimum) distribution, and $1 - e^{-(s_N/\sigma)^m}$ for $\sigma \in (-\infty, 0)$, known as the Fréchet (1927) (minimum) distribution ($s_N = \text{constant}$); Ang and Tang (1984), Soong (2004). Gumbel and Fréchet distributions cannot apply to strength because they govern the minimum as $\sigma \rightarrow -\infty$ and have infinite negative tails.

Thus, the Weibull distribution appears to be the only one mathematically acceptable for brittle structures as well as large enough quasibrittle structures, in which the failure of one small elementary volume of material causes the whole structure to fail. By contrast, the ductile (or plastic) failures must exhibit the Gaussian distribution. This follows by applying the central limit theorem to the plastic limit state in which the load is a sum of many random contributions from all the material elements along the failure surface. The Gaussian (normal) distribution has sometimes been replaced with lognormal, citing the

impossibility of negative strength values. However, this argument is false since, according to the central limit theorem, the negative strength values must always lie beyond the reach of the Gaussian core of pdf. Besides, the lognormal distribution has the wrong skewness, opposite to Weibull. Moreover, a lognormal distribution would mean that the load is a product, rather than a sum, of the contributions from all the elements along the surface, an obvious impossibility. Thus, the log-normal distribution has no place in strength statistics.

Note that all the extreme value distributions presume the elemental properties to be statistically independent (uncorrelated). This is always a good enough hypothesis for structures sufficiently larger than the autocorrelation length l_a of the strength field, although a rescaled mean strength of RVE is needed. But if l_a can be taken equal to the RVE size l_0 , which seems to be quite logical, no rescaling is needed.

If material failure in tension is considered, Eq. (19) is contingent upon the assumption that the random material strength is the same for each spatial direction, i.e., that the strengths in the three principal stress directions are perfectly correlated. Then it is justified to interpret σ in Eq. (19) as the positive part of the maximum principal nonlocal stress at each continuum point. However, if the random strengths in the principal directions at the same continuum point were statistically independent, then σ in Eq. (19) would have to be replaced by $\sum_{I=1}^3 \bar{\sigma}_I$ where $\bar{\sigma}_I$ are the positive parts of the principal nonlocal stresses at that point.

If the material characteristic length l_0 is not negligible compared to D , then the structure inevitably exhibits a combined statistical-energetic size effect, and if D is not $\gg l_0$ then the energetic part will dominate. This can generally be captured by the nonlocal Weibull theory (Bažant and Xi, 1991), in which the material failure probability depends not on the continuum stress at a given point \mathbf{x} but on the nonlocal strain $\hat{\varepsilon}(\mathbf{x})$ at that point, defined by spatial averaging of the positive part of the maximum principal local strain $\varepsilon(\mathbf{x})$ over a neighborhood of size ℓ surrounding point \mathbf{x} . Eq. (10) is then generalized as

$$P_f = 1 - \exp \left[- \int_V \left(\frac{E \hat{\varepsilon}(\mathbf{x})}{s_0} \right)^m \frac{dV(\mathbf{x})}{l_0^{n_d}} \right]. \quad (24)$$

This formulation becomes essentially equivalent to the classical Weibull theory, Eq. (10), when $\ell \leq l_0$, and becomes identical when $D \gg l_0$ and $D \gg \ell$. The nonlocal averaging makes the spatial concentration of failure probability an autocorrelated random field with autocorrelation length l_a equal to ℓ . Although l_a could, in theory, differ from ℓ , it seems reasonable to assume that $l_a \approx \ell$.

The statistical-energetic size effect on the mean of σ_N can be approximately described as (Bažant, 2004a, b; Bažant and Novák, 2001; Bažant et al. 2005b)

$$\sigma_N = A(\vartheta^{m_d/m} + r\kappa\vartheta)^{1/r}, \quad \vartheta = B(1 + D/\eta l_0)^{-1}, \quad (25)$$

where $n_d, m, r, \kappa, \eta, A, B, l_0 = \text{constants}$. This formula was derived by asymptotic matching of the first two terms of the large-size asymptotic expansion of Eq. (24) in powers of $1/D$ with the first two terms of the small-size asymptotic expansion of the cohesive crack model in powers of D (Bažant, 2004a, b).

7. Strength distribution of fiber bundle (parallel coupling) model

Another basic statistical model is the fiber bundle (or parallel coupling) model (Fig. 4b). Various hypotheses of load sharing after fiber break are found in the literature, but the

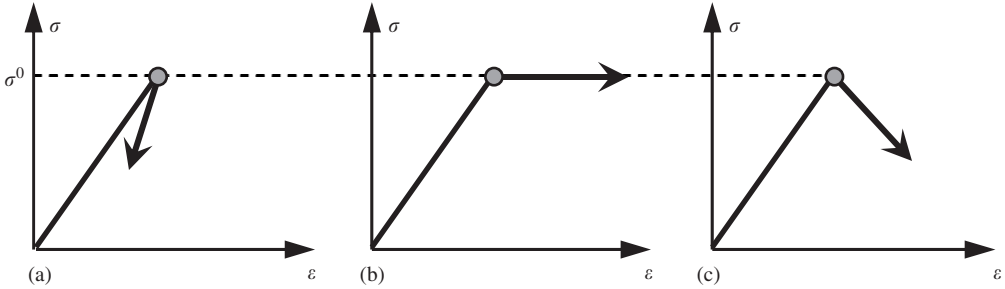


Fig. 5. Post-peak behavior of fibers (a) brittle; (b) plastic; (c) softening.

only physically most meaningful approach is to deduce load sharing from the physical fact that all the fibers are subjected to the same strain ϵ . The fibers are numbered as $k = 1, 2, \dots, n$ in the order of increasing random values of their strengths σ_k . Each fiber is assumed to have the same cross section A_f , same elastic modulus E_f and same cdf $F(\sigma)$ of its strength, and to respond elastically until its strength limit is reached. Two types of fiber behavior after reaching the strength limit are easy to analyze: (a) brittle, in which case the stress drops suddenly to zero, and (b) plastic, in which case the fiber extends at constant stress σ° (Fig. 5). A more realistic post-peak behavior is gradual softening, but it is harder to analyze.

7.1. Brittle bundle

When the j th fiber is about to break, fibers $k = 1, 2, \dots, j - 1$ are already broken. Because the unbroken fibers $k = j, j + 1, j + 2, \dots, n$ (whose number is $n - j + 1$) have the same strain ϵ , the load applied on the bundle is shared equally among all the unbroken fibers and their stress is $\sigma_k = E_f \epsilon$ (for this reason, the brittle fiber bundle is also called the equal-load-sharing model). Consequently, the average stress carried by the whole bundle is $(n - j + 1)\sigma_j/n$, and its maximization yields the bundle strength

$$\sigma = \frac{1}{n} \max_{\epsilon} \sum_{k=1}^n H(\sigma_k - E_f \epsilon) E_f \epsilon = \frac{1}{n} \max_j [(n - j + 1)\sigma_j], \tag{26}$$

where $H =$ Heaviside step function. The bundle strength can also be written as $\sigma = n^{-1} \sum_{k=u}^n E_f \epsilon = [1 - (u - 1)/n] E_f \epsilon$, in which $u = j$ -value for which the last expression is maximized. This shows that the randomness of bundle strength is caused by randomness of the maximizing ratio $\lambda = u/n$ and of the corresponding strain ϵ . The cdf of strength σ of a bundle with n fibers can be exactly computed from Daniels' (1945) recursive formula:

$$G_n(\sigma) = \sum_{k=1}^n (-1)^{k+1} \binom{n}{k} F^k(\sigma) G_{n-k} \left(\frac{n\sigma}{n-k} \right) \quad \text{where} \quad \binom{n}{k} = \frac{n!}{k!(n-k)!}, \tag{27}$$

here $F^k(\sigma) = [F(\sigma)]^k$; $\sigma \geq 0$, $G_0(\sigma) = 1$, $G_n(\sigma)$ is the cdf of strength σ of the whole bundle with n fibers (this equation, though, is unusable for about $n > 75$ because of accumulation of round-off errors).

For large n , the fiber strength values are almost continuously distributed. So, for $n \rightarrow \infty$, the area fraction occupied by unbroken fibers when the fiber of strength σ is breaking is $1 - F(\sigma)$, and the stress carried by the bundle is $\sigma = E_f \epsilon [1 - F(E_f \epsilon)]$. From the

condition $d\sigma/d\varepsilon = 0$, the value $\sigma = \sigma^* = E_f \varepsilon^*$ for which this expression attains a maximum can be easily determined. Since the pdf of infinite bundle is symmetric (Daniels, 1945), the maximum must be equal to the mean strength of the bundle, which is $\mu_\sigma = \sigma^*[1 - F(\sigma^*)]$.

Daniels (1945) proved that, for large n , the variance of the total load on the bundle approaches $n\sigma^{*2}F(\sigma^*)[1 - F(\sigma^*)]$. It follows that the CoV of the strength of a large bundle has the asymptotic approximation

$$\omega_\sigma \approx \rho_0 n^{-1/2} \quad \text{with } \rho_0 \approx \sqrt{F(\sigma^*)/[1 - F(\sigma^*)]} \quad (\text{for large } n), \tag{28}$$

where $\rho_0 = \text{constant}$. Hence, ω_σ vanishes for $n \rightarrow \infty$. In other words, the strength of an infinite bundle is deterministic. So (unlike the chain of many elements), the number of elements (or fibers) in the bundle must be finite and the question is how many of them should be considered. It will be shown that this number cannot exceed the value of Weibull modulus m of a RVE.

A question crucial for reliability of very large structures is the shape of the far-left tail lying outside the Gaussian core of the pdf of bundle strength when n is finite. Obviously, the left tail cannot be Gaussian because a Gaussian cdf (i.e., the error function) has an infinite negative tail whereas the bundle strength cannot be negative. The distance from the mean μ_σ to the point $\sigma = 0$, which is a point sure to lie beyond the Gaussian core, may be written as $\Delta\sigma_{nG} = \mu_\sigma = \delta_\sigma/\omega_\sigma = (\delta_\sigma/\rho_0)\sqrt{n}$, where $\delta_\sigma = \omega_\sigma \mu_\sigma = \text{standard deviation of bundle strength}$. The spread $\Delta\sigma_G$ of the Gaussian core (i.e., the distance from the mean to the end of Gaussian core) must obviously be smaller than this; it is found to be also proportional to \sqrt{n} , i.e.,

$$\Delta\sigma_G = \gamma_G \delta_\sigma \sqrt{n}, \tag{29}$$

where γ_G is some constant less than $1/\rho_0$. Smith (1982) showed that Daniels' Gaussian approximation to the cdf of bundle has the convergence rate of at least $O(n^{-1/6})$, which is a rather slow convergence, and proposed an improved Gaussian approximation with a mean depending on n , for which the convergence rate improves but still is not guaranteed to be better than $O(n^{-1/3}(\log n)^2)$.

Of interest here is the case in which the strength of each fiber has a power-law left tail, of some exponent p . Then the cdf of strength of brittle bundle has also a power-law tail, and its exponent is np .

This important property is revealed by Weibull-scale plots of computer simulations of cumulative histograms according to Eq. (27) (Fig. 6(a)), and may be easily proven by induction from Eq. (27). Set $F(\sigma) = \sigma^p$. For one fiber, $n = 1$, this property is true because $G_1(\sigma) = (-1)^2 \binom{1}{1} F^1(\sigma) G_0 = (\sigma^p)^1$. Now assume this property to be true for the cdf of all bundles with up to $n - 1$ fibers, i.e., $G_k(\sigma) = (\sigma/s_k)^{kp}$ for $k = 1, 2, \dots, n - 1$. Then use Eq. (27) for a bundle with n fibers. Noting that $F^k(\sigma) = \sigma^{kp}$, one gets from (27)

$$\begin{aligned} G_n(\sigma) &= \sum_{k=1}^n (-1)^{k+1} \binom{n}{k} \sigma^{kp} G_{n-k} \left(\frac{n\sigma}{n-k} \right) \\ &= (-1)^{n+1} \binom{n}{n} \sigma^{np} G_0 + \sum_{k=1}^{n-1} (-1)^{k+1} \binom{n}{k} \sigma^{kp} \left(\frac{n\sigma}{(n-k)s_{n-k}} \right)^{(n-k)p} \\ &= \left[(-1)^{n+1} G_0 + \sum_{k=1}^{n-1} (-1)^{k+1} \binom{n}{k} \left(\frac{n}{(n-k)s_{n-k}} \right)^{(n-k)p} \right] \sigma^{np} = \left(\frac{\sigma}{s_n} \right)^{np} \end{aligned} \tag{30}$$

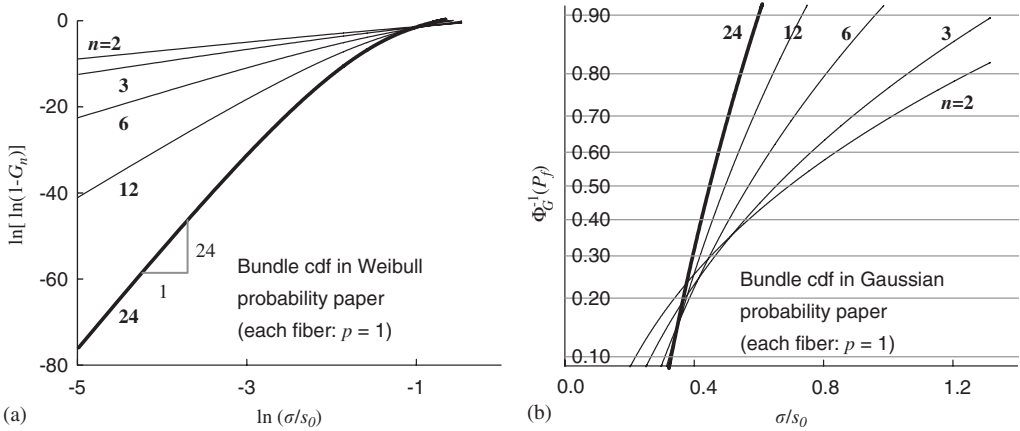


Fig. 6. Strength cdf of elastic–brittle bundles with n fibers, in which each fiber has exponential strength distribution; (a) curves of $\log(P_T)$ versus $\log \sigma$ for fiber bundles with increasing n , in which a straight line of slope p represents a power law of exponent p ; (b) exact cdf of fiber bundle with 24 fibers, plotted on Gaussian probability paper (deviation from straight line is a deviation from Gaussian pdf).

(because all the powers of σ are found to be the same); s_n is a factor independent of σ . (By induction based on the set theory, this property was previously proven for brittle bundles by Harlow et al., 1983; see also the works of Phoenix et al., 1997.)

Now it is clear that parallel couplings can raise the power-law tail exponent from 1 on the nano-scale to any value, m , on the RVE scale. But will this yield a realistic length of the power-law tail?

To check it, let us use Taylor series expansion of the Weibull cdf; $F_{wb}(\sigma) = (\sigma/s_1)^p (1 - \xi/2! + \xi^2/3! - \xi^3/4! + \dots)$ where $\xi = (\sigma/s_1)^p$. Taking only the first two terms of expansion, we obtain $F(\sigma) = (\sigma/s_1)^p (1 - \sigma^p/t_1)$ and $G_k(\sigma) = (\sigma/s_k)^{kp} (1 - \sigma^p/t_k)$ for $k = 1, 2, \dots, n-1$ where s_1, s_k, t_k are constants and $t_1 = 2^{1/p} s_1$. Parameters $t_1^{1/p}$ and $t_k^{1/p}$ describe the vertical deviations from power-law tail, with $d_1 = t_1(\varepsilon)^{1/p}$ and $d_k = t_k(\varepsilon)^{1/p}$ characterizing the horizontal length of tail up to the deviation of $(100\varepsilon)\%$ from the power law.

One may now substitute these expressions into Eq. (27) and use binomial expansions for powers of a sum; this yields

$$\left(\frac{\sigma}{s_n}\right)^{np} \left[1 - \left(\frac{\sigma}{t_n}\right)^p\right] \approx \sum_{k=1}^{n-1} (-1)^{k+1} \binom{n}{k} \left(\frac{\sigma}{s_1}\right)^{kp} \left[1 - k \left(\frac{\sigma}{t_1}\right)^p\right] \left(\frac{n\sigma}{j s_j}\right)^{jp} \left[1 - \left(\frac{n\sigma}{j t_j}\right)^p\right] + (-1)^{n+1} \left(\frac{\sigma}{s_1}\right)^{np} \left[1 + n \left(\frac{\sigma}{t_1}\right)^p\right], \tag{31}$$

where $j = n - k$. For this equation to be valid for every small σ , the coefficients of the combined terms with σ^{np} and σ^{np+1} must vanish. The former yields Eq. (30), and the latter yields

$$\frac{t_1}{t_n} = \left\{ \sum_{k=1}^{n-1} (-1)^{k+1} \binom{n}{k} \left(\frac{n s_1}{j s_j}\right)^{jp} \left[k + \left(\frac{n t_1}{j t_j}\right)^p \right] + (-1)^{n+1} n \right\}^{1/p} \left(\frac{s_n}{s_1}\right)^n. \tag{32}$$

Table 1

Ratio of the length nd_n of power-law tail for total load of an elastic–brittle bundle to tail length t_1 of one fiber

	$p = 1$	2	4	6	8	12
$n = 2$	0.600	0.858	0.978	0.996	0.999	1.000
3	0.462	0.807	0.973	0.996	0.999	1.000
4	0.391	0.780	0.972	0.996	0.999	1.000
6	0.316	0.752	0.971	0.996	0.999	1.000
12	0.232	0.724	0.970	0.999	0.999	1.000
24	0.181	0.710	0.970	0.999	0.999	1.000

Table 2

Extent of power-law tail probabilities for an elastic–brittle bundle with a tail exponent of 24

s_1/s_n	t_1/t_n	p	n	d_n/d_1	P_m/P_{t1}	P_m
1.00	1.00	24	1	1.000	1.00×10^{-00}	3.00×10^{-01}
1.46	2.00	12	2	0.500	1.00×10^{-04}	5.50×10^{-05}
1.78	3.00	8	3	0.333	1.00×10^{-07}	1.30×10^{-07}
2.05	4.02	6	4	0.249	1.00×10^{-09}	7.89×10^{-10}
2.53	6.18	4	6	0.162	1.00×10^{-12}	3.76×10^{-13}
2.98	8.74	3	8	0.114	1.34×10^{-15}	4.02×10^{-16}
3.83	16.57	2	12	0.060	9.43×10^{-22}	2.83×10^{-22}
6.23	132.79	1	24	0.008	1.21×10^{-44}	3.62×10^{-45}

This is a recursive linear equation for t_1/t_n . Numerical evaluation of nd_n/d_1 indicates that, for $n = 2$ to 24 fibers, the total load of the whole bundle remains about constant for $p \geq 3$ (Table 1). This conclusion is based on comparing d_n/d_1 for bundles with a different number of fibers of the same tail exponent for each fiber (Table 1), e.g. ($p = 3, n = 2$), ($p = 3, n = 3$), ($p = 3, n = 4$), etc., and not for bundles with the same tail exponent for the whole bundle (Table 2), e.g. ($p = 1, n = 24$), ($p = 2, n = 12$), ($p = 3, n = 8$), etc.

Since d_n is the average strength per one of n fibers, the extent of the power-law tail of d_n of the bundle strength must decrease, in terms of stress, roughly as $1/n$.

7.2. Plastic bundle

If the fibers deform plastically, the maximum load of the bundle is the sum of n independent (uncorrelated) random variables σ_k ($k = 1, 2, \dots, n$). This is a classical problem of statistics, which is completely understood (and is simpler than that of a brittle bundle). The central limit theorem of the theory of probability (e.g., Bulmer, 1967; Feller, 1957; Soong, 2004) states that (if all σ_k have a finite variance) the sum $Y = \sum_{k=1}^n \sigma_k$ for $n \rightarrow \infty$ converges, except in the tails, to the Gaussian pdf (and does so with absolute error $O(n^{-1/2})$).

The distance from the mean of a sum to the tail is known to be proportional to $\delta\sqrt{n}$ (e.g., Bouchaud and Potters, 2000) where δ is the standard deviation of the sum. To simply understand why, note that, by elementary rules (e.g., Haldar and Mahadevan, 2000,

p. 150), the mean and variance of the maximum load of the bundle are $\mu_n = n\mu_\sigma$ and $s_n^2 = ns_\sigma^2$ where μ_σ and s_σ^2 are the mean and variance of σ_k . If all σ_k are nonnegative, μ must be nonnegative, too, even though the Gaussian pdf has an infinite negative tail. Of course, the Gaussian pdf of tensile strength cannot apply within the range of negative σ ; hence, the Gaussian core cannot reach farther from the mean μ_n than to the distance of rs_n where $r = n\mu_\sigma/\sqrt{ns_\sigma^2} = \omega_n^{-1} = \omega_0^{-1}\sqrt{n}$, with ω_0 denoting the CoV of one fiber.

The tail outside the Gaussian core and the tails of σ_k are known to be of the same type (Bouchaud and Potters, 2000); i.e., if the tail of fibers is a power-law, so is the tail of the mean. To explain this and other tail properties, consider a bundle of two plastic ‘fibers’ with stresses y and z , and tail cdf of strength:

$$G(y) = \left(\frac{y}{y_0}\right)^{jp} \left[1 - \left(\frac{y}{t_j}\right)^p\right], \quad H(z) = \left(\frac{z}{z_0}\right)^{kp} \left[1 - \left(\frac{z}{t_k}\right)^p\right], \tag{33}$$

where j, k, p, y_0, z_0 are positive constants, and parameter t defines the power-law tail length such that (100 ε)% deviations from each power-law tail occur at $d = t\varepsilon^{1/p}$ (note that when $j = k = 1$, $G(y)$ and $H(z)$ describe the first two terms of the expansion of Weibull cdf). By differentiation, the corresponding pdf tails are

$$g(y) = \frac{jp}{y_0} \left(\frac{y}{y_0}\right)^{jp-1} \left[1 - \left(\frac{y}{t_j}\right)^p\right], \quad h(z) = \frac{kp}{z_0} \left(\frac{z}{z_0}\right)^{kp-1} \left[1 - \left(\frac{z}{t_k}\right)^p\right], \tag{34}$$

where

$$t'_j = t_j \left(\frac{jp}{jp+p}\right)^{1/p}, \quad t'_k = t_k \left(\frac{kp}{kp+p}\right)^{1/p}. \tag{35}$$

The maximum load on the bundle is $x = y + z$. Load x can be obtained by all possible combinations of forces y and $z = x - y$ in the first and second fibers, which both must be at their strength limit if the bundle load is maximum. So, according to the joint probability theorem, the pdf of the sum x is

$$\begin{aligned} f(x) &= \int_0^x g(y)h(x-y) dy \\ &= jkp^2 y_0^{-jp} z_0^{-kp} \int_0^x y^{jp-1} (x-y)^{kp-1} \left[1 - \left(\frac{y}{t'_j}\right)^p\right] \left[1 - \left(\frac{x-y}{t'_k}\right)^p\right] dy. \end{aligned} \tag{36}$$

Although the standard approach in the theory of probability would be to take the Laplace transform of the above convolution integral and later invert it, a conceptually simpler power series approach will suffice for our purpose. We expand $(x-y)^{kp-1}$ and $(x-y)^p$ according to the binomial theorem and, upon integrating, we retain only two leading terms of the power series expansion of $f(x)$. This yields

$$f(x) \approx \frac{jkp^2 C'_0}{y_0^{jp} z_0^{kp}} \left[1 - C'_p \left(\frac{x}{t'_j}\right)^p - C'_q \left(\frac{x}{t'_k}\right)^p\right] x^{jp+kp-1} \quad (\text{error} \propto x^{(j+k+2)p-1}), \tag{37}$$

where

$$C'_0 = \frac{\Gamma(jp)\Gamma(kp)}{\Gamma(jp+kp)}, \quad C'_p = \frac{\Gamma(jp+kp)\Gamma(p+jp)}{\Gamma(jp)\Gamma(jp+kp+p)}, \quad C'_q = \frac{\Gamma(jp+kp)\Gamma(p+kp)}{\Gamma(kp)\Gamma(jp+kp+p)}. \tag{38}$$

The corresponding cdf of the maximum load on the bundle of two fibers is

$$F(x) \approx \left(\frac{x}{x_0}\right)^{(j+k)p} \left[1 - \left(\frac{x}{t^*}\right)^p\right], \tag{39}$$

where

$$x_0^{-(j+k)p} = \frac{C'_0}{y_0^j z_0^k} \frac{jkp}{(j+k)}, \quad (t^*)^{-p} = \frac{C'_p(j+1)(j+k)}{j t_j^p (j+k+1)} + \frac{C'_q(k+1)(j+k)}{k t_k^p (j+k+1)}. \tag{40}$$

So we conclude that the exponents of fiber tails in a plastic bundle are additive, while the length of the power-law tail of the cdf of the total load of the bundle decreases from $d_1 = t_1 \varepsilon^{1/p}$ to $d_m = t^* \varepsilon^{1/p}$. In the case of fibers with $p = 1$, a bundle of three fibers is a coupling of one fiber with a bundle of two fibers, which gives $d_m/d_1 = 0.667$; a bundle of four fibers is a coupling of one fiber with a bundle of three fibers, which gives $d_m/d_1 = 0.625$, etc., and for 24 fibers $d_m/d_1 = 0.521$.

The cdf of the average strength of each fiber is simply a horizontal scaling of the cdf for the total load on the bundle, and so Eq. (39) can be written in terms of σ :

$$F(\sigma) = \left(\frac{n\sigma}{x_0}\right)^{(j+k)p} \left[1 - \left(\frac{n\sigma}{t^*}\right)^p\right] = \left(\frac{\sigma}{s_n}\right)^{np} \left[1 - \left(\frac{\sigma}{t_n}\right)^p\right], \tag{41}$$

where $s_n = x_0/n$, $t_n = t^*/n$ and $n = j + k$. So we see that the total load, as well as the average strength of the bundle, has a cdf tail with exponent np , which is the same as for a brittle bundle. The length of the power-law tail of the cdf of the strength of a bundle (i.e., the load per fiber), which is $d_n = d_m/n$, gets changed, for $\varepsilon = 0.15$, by factors $0.667/3 = 0.222$ and $0.521/24 = 0.022$, respectively, with $p = 1$.

In general, the length of the power-law tail of the cdf for elastic–plastic bundle is about 2 to three times longer than the corresponding length for elastic–brittle bundle (Table 3).

7.3. Extent of tail in terms of failure probability

The shortening of power-law tail with increasing number of fibers in a bundle may be modest in terms of stress, but in terms of failure probability P_f it is drastic if n not very

Table 3
Extent of power-law tail probabilities for an elastic–plastic bundle with a tail exponent of 24

s_1/s_n	t_1/t_n	p	n	d_n/d_1	P_m/P_{t1}	P_m
1.00	1.00	24	1	1.000	1.00×10^{-00}	3.00×10^{-01}
1.08	1.27	12	2	0.787	1.00×10^{-02}	3.00×10^{-03}
1.15	1.49	8	3	0.672	2.40×10^{-04}	7.20×10^{-05}
1.22	1.72	6	4	0.583	7.79×10^{-06}	2.34×10^{-06}
1.35	2.27	4	6	0.440	1.00×10^{-08}	3.01×10^{-09}
1.48	3.04	3	8	0.329	7.39×10^{-12}	2.22×10^{-12}
1.73	5.65	2	12	0.177	8.37×10^{-19}	2.51×10^{-19}
2.45	46.08	1	24	0.022	2.41×10^{-43}	7.23×10^{-44}

small. The P_f value at the terminal point of power-law tail gets reduced in the ratio:

$$\rho_P = \frac{P_{tn}}{P_{t1}} = \frac{(d_n/s_n)^{np}}{(d_1/s_1)^{np}} = \left(\frac{t_n s_1}{t_1 s_n} \right)^{np} (2\varepsilon)^{n-1}. \quad (42)$$

Thus, for the brittle or plastic case, respectively, we have, in terms of P_f , the following reduction ratios for the tail terminal point:

$$\text{for two fibers and } p = 12: \quad \rho_P = 1.8 \times 10^{-4} \text{ or } 1.0 \times 10^{-2},$$

$$\text{for three fibers and } p = 8: \quad \rho_P = 4.3 \times 10^{-7} \text{ or } 2.4 \times 10^{-4},$$

$$\text{for six fibers and } p = 4: \quad \rho_P = 1.3 \times 10^{-12} \text{ or } 1.0 \times 10^{-8},$$

$$\text{for 24 fibers and } p = 1: \quad \rho_P = 1.2 \times 10^{-44} \text{ or } 2.4 \times 10^{-43}. \quad (43)$$

Obviously, for the same number of fibers, the shortening of the power-law tail is for brittle fibers (Table 2) much stronger than for plastic fibers (Table 3) in small bundles, but not in large bundles. For softening fibers (Fig. 5(c)), intermediate behavior may be expected.

According to the aforementioned values, not even two fibers with $m = 24$ power-law tail up to $P_{t1} = 0.3$ could produce a power-law tail of a bundle reaching up to $P_m = 0.003$, which is the tail length needed to satisfy Hypothesis II, because analysis of chains with various numbers of RVEs shows that a power law-tail of one RVE reaching up to $P_{t1} = 0.003$ produces a Weibull cdf up to $P_m = 0.8, 0.9$ and 0.95 for 500, 750 and 1000 RVEs, respectively. When the number of RVEs > 500 , the cdf on the Weibull probability paper is visually hardly distinguishable from a straight line (Fig. 8(b)).

Therefore, if the tail of the bundle should extend up to $P_f = 0.003$, it is necessary for the cdf of two plastic fibers in the bundle to be Weibull up to at least $P_1 = 0.3$ (computer simulations, too, confirm it). The power-law tail of the cdf of bundle strength, terminates at

$$P_m \approx \varepsilon^n \left(\frac{t_n}{s_n} \right)^{np} = P_{t1}^n \left(\frac{s_1 t_n}{s_n t_1} \right)^{np}, \quad (44)$$

where $P_{t1} = \varepsilon(t_1/s_1)^p$ = failure probability at the terminal point of the power-law tail of one fiber. For a bundle with plastic fibers, the ratio $(t_n s_1)/(t_1 s_n)$ decreases approximately as $n^{-1/p}$, with an error of $< 3\%$, which leads to a shrinking of P_m as $(P_{t1}/n)^n$. To wit, if the power-law tail of one fiber ends at $P_{t1} = 0.3$, the tails of bundles with a tail exponent of $m = np = 24$ for three or eight fibers terminate at $P_f \approx 7.2 \times 10^{-5}$ or 2.2×10^{-12} . Obviously, the power-law tail of the strength of any bundle with more than about three fibers is, from the practical viewpoint, nonexistent. Accurate computer simulations confirm that (see Table 3).

From this we may conclude that if the power-law tail of one fiber strength terminates at $P_{t1} = 0.3$, then the tail of bundle strength (total load per fiber) with tail exponent 24, terminates at $P_f = 3.0 \times 10^{-3}, 7.2 \times 10^{-5}$ and 7.2×10^{-44} , respectively, if $n = 2, 3$ or 24. The last value is so small that the power-law tail can have no effect in reality.

7.4. Basic properties of softening, brittle and plastic bundles

Of main practical interest is a bundle of softening fibers. Because the softening is intermediate between plastic and brittle responses (Fig. 5(c)), those properties that are common to both brittle and plastic bundles may be assumed to hold also for bundles with softening fibers. They may be summarized as follows.

Theorem 1. *For brittle, plastic, and probably also softening, fibers, the exponents of power-law tail of cdf of fibers in a bundle (or parallel coupling) are additive. The power-law tail exponent of strength cdf of a chain is the smallest power-law tail exponent among all links in the chain (or series coupling). Parallel coupling reduces the length of power-law tail of cdf (within one order of magnitude for up to 10 fibers, and up to two orders of magnitude for up to 24 fibers). But the extent of the tail in terms of failure probability can decrease by many more orders of magnitude when the power-law tail exponent of the bundle is high. If the power-law tail exponent of each fiber is high (> 10), it is possible to couple in parallel no more than two non-brittle (plastic or, probably, softening) fibers if a nonnegligible power-law tail of a bundle should be preserved.*

8. Extreme value statistics of RVE and of quasibrittle structure

According to Eq. (7), the failure probability of a chain of N_{eq} identical links with failure probability $P_1(\sigma)$ can be exactly calculated as $P_f(\sigma) = 1 - [1 - P_1(\sigma)]^{N_{\text{eq}}}$. Hence,

$$N_{\text{eq}} = \frac{\log(1 - P_f)}{\log(1 - P_1)}. \quad (45)$$

If the chain of N links is characterized by Weibull cdf up about $P_f = 0.80$, the whole experimental cumulative histogram with typical scatter is, on the Weibull probability paper, visually indistinguishable from Weibull cdf. If the limit of power-law tail of the cdf of one link (one RVE) in a chain is $P_{f1} = 0.003$ (which is a tail hardly detectable in experiments), the equivalent number N_{eq} of RVEs in the structure (or links in the chain) must be, according to Eq. (45), approximately

$$N_{\text{eq}} \geq 500 \quad (46)$$

in order to produce for the chain a cdf indistinguishable from Weibull. For concrete specimens, as it appears, statistical samples with $N_{\text{eq}} > 500$ do not exist. However, test data for fine-grained ceramics cover this kind of size, and they show a distinctly Weibull cdf (e.g., Weibull, 1939; Bansal et al. 1976a, b; Ito et al., 1981; Katayama and Hattori, 1982; Matsusue et al., 1982; Soma et al., 1985; Ohji, 1988; Amar et al., 1989; Hattori et al., 1989; Brühner-Foit and Munz, 1989; Quinn, 1990; Quinn and Morrell, 1991; Katz et al., 1993; Gehrke et al., 1993; Danzer and Lube, 1996; Sato et al., 1996; Lu et al., 2002a; Santos et al., 2003). This justifies Hypothesis II. Therefore, it is logical to assume that a RVE of any quasibrittle material that becomes brittle on the large scale of application should have a power-law tail extending roughly up to $P_{f1} \approx 0.003$.

One microcrack in a RVE, or too few of them, would not cause the RVE, and thus the whole structure, to fail (which is, of course, why the RVE cannot be assumed to behave

statistically as a chain). Rather, a certain number of separate microcracks must form to cause the RVE to fail, which is statistically the same situation as in a bundle of parallel fibers. This number, n , obviously depends on the packing of dominant aggregate pieces in concrete, or the packing of dominant grains in a ceramic or rock, or generally the packing of dominant heterogeneities in the material.

So, the RVE must be considered to behave statistically as a bundle (Fig. 4(b)), and the structure (of positive geometry) as a chain of such bundles (Fig. 4(d)). However, can the RVE be modelled by Daniels' bundle of fibers, or is it necessary to consider that the elements of the bundle consist of chains, sub-bundles, sub-chains, sub-sub-bundles, etc.? It is argued that the latter must be the case.

As additional support for the hypothesis that a RVE of quasibrittle material must behave as a bundle (series coupling), two points should be noted: (i) If the alleged RVE behaved as a chain (series) coupling, the failure would localize into an element of the chain and the actual RVE would be smaller than the alleged RVE. (ii) Since concrete microstructure is brittle, the cdf of strength of small laboratory specimens could not appear as Gaussian (Hypothesis III) if parallel coupling statistics did not apply. Yet majority of experiments for concrete show this cdf to be in fact approximately Gaussian, except in the undetectable tails (Julian, 1955; Shalon and Reintz, 1955; Rüsçh et al., 1969; Erntroy, 1960; Neaman and Laguros, 1967; Metcalf, 1970; Mirza et al., 1979; Bartlett and MacGregor, 1996; FHWA, 1998; Chmielewski and Konopka, 1999).

Consider now a chain of RVEs (Fig. 4(f)). The cdf of strength of each RVE has a power-law cdf tail, and so a long enough chain will follow the Weibull cdf. How many links (i.e., RVEs) are needed to attain Weibull distribution for the whole chain (or structure)?

If the structural model were a chain of bundles (Harlow et al., 1983), each bundle would have, for concrete, 24 parallel fibers of tail exponent 1, and, as has been shown, this would yield for each bundle a tail extending only up to the probability $P_f \approx 10^{-45}$. This means that the chain would have to consist of about 10^{47} bundles for the Weibull distribution to get manifested (a chain of that many RVEs, each of the size of 0.1 m, would have to reach beyond the most distant galaxies!). So, if each RVE were modelled by Daniels' bundle of m fibers with activation energy based cdf ($p = 1$), the Weibull cdf would never be observed in practice. Yet it is (Weibull, 1939).

Based on experience (Weibull, 1939), it may be assumed (Hypothesis II) that the cdf of a positive geometry structure in which the number N of RVEs is about 1000 should be much closer to Weibull than to Gaussian distribution (whether N should rather be 10^4 is, of course, debatable, but it definitely cannot be orders of magnitude larger). To obtain for such N a cdf that is experimentally indistinguishable from Weibull, the power-law tail of cdf of each RVE must, according to Eq. (45), extend up to at least $P_f \approx 0.003$. To this end, the bundle with $m = 24$ must contain no more than two parallel fibers (each of which, with tail exponent 12), must almost completely follow Weibull distribution, and must be of plastic or softening type.

A tail below $P_f = 0.003$ does not get manifested in graphical cumulative histograms and cannot be directly confirmed by any of the existing test data from small laboratory specimens that are not much larger than a RVE (a cumulative histogram of at least 10^4 identical tests would be needed to reveal such a tail on Weibull probability paper). Neither can the Weibull cdf for 1000 RVEs be checked for concrete, because large enough

specimens have not been tested. Nevertheless, confirmation can be obtained from the existing experimental data for specimens of fine-grained ceramics, which contain at least 1000 RVEs. Indeed, they follow the Weibull distribution closely (Weibull, 1939; Bansal et al. 1976a, b; Ito et al., 1981; Katayama and Hattori, 1982; Matsusue et al., 1982; Soma et al., 1985; Ohji, 1988; Amar et al., 1989; Hattori et al., 1989; Brühner-Foit and Munz, 1989; Quinn, 1990; Quinn and Morrell, 1991; Katz et al., 1993; Gehrke et al., 1993; Danzer and Lube, 1996; Sato et al., 1996; Lu et al., 2002a; Santos et al., 2003).

The length of power-law tail of the cdf of RVE is found to strongly depend on whether each of the parallel fibers is brittle or plastic. Brittle fibers never give a sufficiently long power-law tail for the cdf of a RVE, even for just two parallel fibers with tail exponent 12 (required to obtain $m = 24$). A long enough power-law tail of RVE, extending up to $P_f = 0.003$ (Hypothesis II), is obtained for a bundle of two plastic fibers, and doubtless also for a bundle of softening fibers with a sufficiently mild softening slope. This has been verified by computer simulations, and also follows from the aforementioned general rules for the length of power-law cdf tails of bundles.

Based on Hypotheses II and III, and within the context of activation energy theory (Hypothesis I), it follows from the foregoing analysis that a power-law tail of exponent such as $m = 24$, extending up to $P_f = 0.003$, can be achieved for an RVE only with a hierarchical statistical model involving both parallel and series couplings, as idealized in Fig. 4(e). The first bundle (parallel coupling) must involve not more than two parallel elements, and each of them may then consist of a hierarchy of sub-chains of sub-bundles of sub-sub-chains of sub-sub-bundles, etc. The load-deflection diagrams of the sub-chains, sub-sub-chains, etc., cannot be perfectly brittle, i.e., must be plastic or softening. If the constituents of the RVE are not plastic, as in the case of concrete, rocks or ceramics, elements behaving plastically are, of course, unrealistic. Hence, the elements of the hierarchical statistical model should in reality be softening. At any scale of microstructure, a softening behavior is engendered by distributed microcracking on a lower-level sub-scale even if every constituent on that sub-scale is brittle.

In the hierarchical statistical model exemplified in Fig. 4(e), the elements of identical power-law tails, coupled in each sub-chain, serve to extend the power-law tail and, if long enough, will eventually produce Weibull cdf while the tail exponent remains unchanged. On the next higher scale, the parallel coupling of two or three of these sub-chains in a sub-bundle will raise their tail exponent by summation but will shorten the power-law tail significantly. Then, on the next higher scale of microstructure, a series coupling of many sub-bundles in a chain will again extend the power-law tail, and a parallel coupling of two of these chains will again raise the tail exponent and shorten the power-law tail significantly, until the macroscale of an RVE is reached.

The actual behavior of a RVE will, of course, correspond to some irregular hierarchical model, such as that shown in Fig. 4(g). In that case, according to the aforementioned basic properties, the exponent of the power-law tail for the RVE, and thus the Weibull modulus of a large structure, is determined by the minimum cross section, defined as the section with the minimum number of cuts of elementary serial bonds that are needed to separate the model into two halves.

Because random variations in the couplings of the hierarchical model for extreme value statistics of RVE must be expected, it would make hardly any sense to compute the structural failure probability directly from activation energy controlled interatomic bonds characterized by power-law cdf tail of exponent 1. Nevertheless, establishing the

hierarchical model that provides a statistical connection of RVE strength to the stress dependence of activation energy barriers of interatomic bonds has five benefits:

1. It proves that the cdf of RVE strength must have a power-law tail.
2. It proves that a sufficiently long tail, extending up to $P_f \approx 0.0001$ – 0.01 , and the Weibull distribution of strength of a large enough structure, are physically justifiable.
3. It proves that the Weibull distribution must have a zero threshold.
4. It provides the dependence of Weibull scale parameter s_0 on temperature T and on characteristic load duration τ (or on the loading rate, which is characterized by $1/\tau$).
5. It indicates that the complicated transition between the power-law tail and the Gaussian core can be considered to be short (because, with only two or three elements coupled in parallel, the power-law tail reaches far enough).

Point 4, according to Eqs. (6) and (10), means that the scaling parameter S_0 of the Weibull cdf of structural strength must depend on absolute temperature T and on load duration τ (or loading rate $1/\tau$), and that the dependence must have the form:

$$S_0 = S_{0r} \frac{T}{T_0} \frac{\phi_b(\tau_0)}{\phi_b(\tau)} e^{(1/T-1/T_0)Q/k}, \quad (47)$$

where T_0 = reference absolute temperature (e.g., room temperature 298°K), τ_0 = reference load duration (or time to reach failure of the specimen, e.g., 1 min), and S_{0r} = reference value of S_0 corresponding to T_0 and τ_0 . The corresponding Weibull cdf of structural strength at any temperature and load duration may be written as

$$P_f(\sigma) = 1 - \exp \left\{ - \left[\frac{\sigma}{S_{0r}} \frac{T_0}{T} \frac{\phi_b(\tau)}{\phi_b(\tau_0)} e^{(1/T_0-1/T)Q/k} \right]^m \right\}. \quad (48)$$

Note, however, that this simple dependence on T is expected to apply only through a limited range of temperatures and load durations. The reason is that the interatomic potential surface typically exhibits not one but many different activation barriers Q and coefficients κ for different atoms and bonds, with different Q and κ dominating in different temperature ranges.

On the atomic scale, which is separated from the RVE scale of concrete by about eight orders of magnitude, the breakage of a RVE must involve trillions of interatomic bond breaks governed by activation energy. Lest one might have doubts about using the activation energy theory to span so many orders of magnitude, it should be realized that there are many other similar examples where the activation energy has been successfully used for concrete, rock, composites and ceramics—e.g., the temperature dependence of fracture energy and of creep rate of concrete (Bažant and Prat, 1988), the effect of crack growth rate on fracture resistance (Bažant and Jirásek, 1993; Bažant, 1995; Bažant and Li, 1997), or the softening–hardening reversal due to a sudden increase of loading rate (Bažant et al., 1995).

Activation energy concepts have been used by Zhurkov (1965) and Zhurkov and Korsukov (1974) in a deterministic theory of structural lifetime as a function of T and σ , which corresponds to replacing Eq. (4) by

$$F(\sigma) = \min[(C_b/2)e^{\kappa\sigma/kT}, 1] \quad \text{for } \sigma \geq 0. \quad (49)$$

The corresponding pdf, however, has a delta-function spike at $\sigma = 0$, which is objectionable. The preceding derivation would lead to this formula if the bond

restorations, governed by activation energy barrier $Q + \kappa\sigma$, were ignored, i.e., if $f_b = e^{-(Q-\kappa\sigma)/kT}$ instead of Eq. (3). As a result, this theory incorrectly predicts a solid to disintegrate within a finite lifetime even if $\sigma = 0$, and it also gives unrealistically short lifetimes for failures at low stress, i.e., for low failure probabilities and for large structures. Especially, Zhurkov's theory is incompatible with Weibull theory and could not be combined with the present analysis.

In a similar way as here, the activation energy concept has more recently been used in probabilistic analysis of the lifetime distribution, based on models of the evolution of defects in parallel coupling systems with various assumed simple load-sharing rules; see Phoenix (1978), Phoenix and Tierney (1983), Phoenix and Smith (1983), Curtin and Scher (1997), Phoenix et al. (1997), and Newman and Phoenix (2001). The temperature and stress dependence of lifetime has been related to the interatomic activation energy through an argument traced to Eyring (1936; also Eyring et al., 1980; Glasstone et al., 1941; Tobolsky, 1960).

9. Grafted Weibull–Gaussian cdf of one RVE

If the RVE of concrete (with $m \approx 24$) were modelled as a bundle of more than two fibers, the transition of its cdf from the Gaussian core to the Weibull (or power-law) tail would occupy several orders of magnitude of P_f . The mathematical formulation of such transition region would be complicated. However, as has already been argued, the bundles and sub-bundles in the hierarchical model for RVE should contain only, near the macroscale, no more than two parallel fibers (with more parallel fibers allowed for scales close to nano, where the tail exponent is low). Consequently, the transition region in terms of P_f must be relatively short, happening within one or two orders of magnitude of P_f .

This permits us to assume, for the sake of simplicity, that the transition occurs approximately within a point, $\sigma_{N,gr}$. In other words, we may assume that a Weibull pdf tail ϕ_W is grafted at one point on the left side onto a Gaussian pdf core ϕ_G (i.e., onto the error function). Such a grafted pdf (Bažant and Pang, 2005b), may be mathematically described as follows:

$$\text{for } \sigma_N < \sigma_{N,gr} : p_1(\sigma_N) = r_f(m/s_1)(\sigma_N/s_1)^{m-1} e^{-(\sigma_N/s_1)^m} = r_f \phi_W(\sigma_N), \quad (50)$$

$$\text{for } \sigma_N \geq \sigma_{N,gr} : p_1(\sigma_N) = r_f e^{-(\sigma_N - \mu_G)^2 / 2\delta_G^2} / (\delta_G \sqrt{2\pi}) = r_f \phi_G(\sigma_N), \quad (51)$$

where μ_G , δ_G = mean and standard deviation of Gaussian core alone; m , s_1 = shape and scale parameters of Weibull tail alone. The cdf of the latter is

$$\text{for } \zeta < \zeta_{gr} : P_1(\zeta) = r_f(1 - e^{-\zeta^m}),$$

$$\text{for } \zeta \geq \zeta_{gr} : P_1(\zeta) = r_f(1 - e^{-\zeta^m}) + \frac{r_f}{\delta_{Gn} \sqrt{2\pi}} \int_{\zeta_{gr}}^{\zeta} e^{-(\zeta' - \mu_{Gn})^2 / 2\delta_{Gn}^2} d\zeta' \quad (52)$$

where

$$r_f = [1 - \Phi_G(\zeta_{gr}) + \Phi_W(\zeta_{gr})]^{-1}. \quad (53)$$

Here $\mu_{Gn} = \mu_G/s_1$; $\delta_{Gn} = \delta_G/s_1$; $\zeta_{gr} = \sigma_{N,gr}/s_1$. r_f is a scaling factor ensuring that the cdf of the Weibull–Gaussian graft be normalized; $\int_{-\infty}^{\infty} \phi(\sigma_N) d\sigma_N = 1$. The far-left tail of cdf of

P_1 is a power law which can be expressed as

$$P_1 \approx r_f(\sigma_N/s_1)^m \quad (\text{for } \sigma_N \rightarrow 0). \tag{54}$$

The scale parameter s_1 used in the grafting method is related to s_0 of Eq. (12) by $s_0 = r_f^{1/m} s_1$. The typical values for r_f range between 1.00 and 1.14, which means that s_0 differs from s_1 by less than 0.5%. In practice, $r_f^{1/m}$ can be taken as 1, and $s_0 = s_1$. But r_f should remain in the formulation of P_1 (Eq. 52), or else an error of up to 12% in the cdf of one RVE is likely.

Both pdfs, as defined in Eqs. (50) and (51), are matched to be continuous at the grafting point, ζ_{gr} . This gives the compatibility condition:

$$\mu_{Gn} = \zeta_{gr} - \delta_{Gn} \{-2 \ln[\sqrt{2\pi m} \delta_{Gn} \zeta_{gr}^{m-1} e^{-\zeta_{gr}^m}]\}^{1/2}. \tag{55}$$

The probability at which the Weibull tail for one RVE ceases to apply lies within the range $P_{gr} = r_f \Phi_W(\zeta_{gr}) \approx 0.0001\text{--}0.01$, and is used to determine the relative length of the Weibull tail ζ_{gr} , to be grafted:

$$\zeta_{gr} = [-\ln(1 - \Phi_W(\zeta_{gr}))]^{1/m}. \tag{56}$$

If one knows the standard deviation of the Gaussian core δ_G and the scale parameter s_1 of the Weibull tail, one can calculate μ_{Gn} from Eq. (55); δ_G can be easily determined from the

Table 4

Mean μ , standard deviation δ , and CoV ω_0 of the grafted distribution for one RVE for various grafting probabilities $\Phi_W(\alpha_{gr})$

P_{gr}	r_f	ζ_{gr}	μ_{Gn}	δ_{Gn}	μ_0/s_1	δ_0/s_1	ω_0
0.001	1.016	0.7493	3.584	1.335	3.640	1.275	0.350
0.001	1.009	0.7496	2.723	0.850	2.746	0.825	0.300
0.001	1.005	0.7496	2.095	0.535	2.103	0.525	0.250
0.001	1.003	0.7499	1.649	0.344	1.653	0.331	0.200
0.001	1.001	0.7499	1.324	0.200	1.325	0.199	0.150
0.001	1.000	0.7499	1.084	0.109	1.085	0.108	0.100
0.003	1.040	0.7838	2.512	0.993	2.599	0.911	0.350
0.003	1.024	0.7843	2.112	0.686	2.152	0.645	0.300
0.003	1.014	0.7846	1.776	0.468	1.793	0.449	0.250
0.003	1.008	0.7848	1.497	0.309	1.504	0.301	0.200
0.003	1.003	0.7850	1.266	0.192	1.268	0.190	0.150
0.003	1.000	0.7851	1.079	0.108	1.080	0.108	0.100
0.005	1.064	0.7999	2.160	0.896	2.275	0.796	0.350
0.005	1.040	0.8007	1.894	0.638	1.951	0.585	0.300
0.005	1.024	0.8012	1.651	0.446	1.677	0.419	0.250
0.005	1.013	0.8015	1.432	0.301	1.443	0.289	0.200
0.005	1.006	0.8018	1.241	0.191	1.245	0.187	0.150
0.005	1.001	0.8020	1.074	0.107	1.075	0.107	0.100
0.010	1.137	0.8212	1.751	0.823	1.940	0.680	0.350
0.010	1.086	0.8227	1.632	0.600	1.730	0.519	0.300
0.010	1.052	0.8238	1.491	0.427	1.538	0.385	0.250
0.010	1.029	0.8246	1.344	0.292	1.363	0.273	0.200
0.010	1.013	0.8251	1.202	0.189	1.209	0.182	0.150
0.010	1.002	0.8255	1.069	0.108	1.070	0.107	0.100

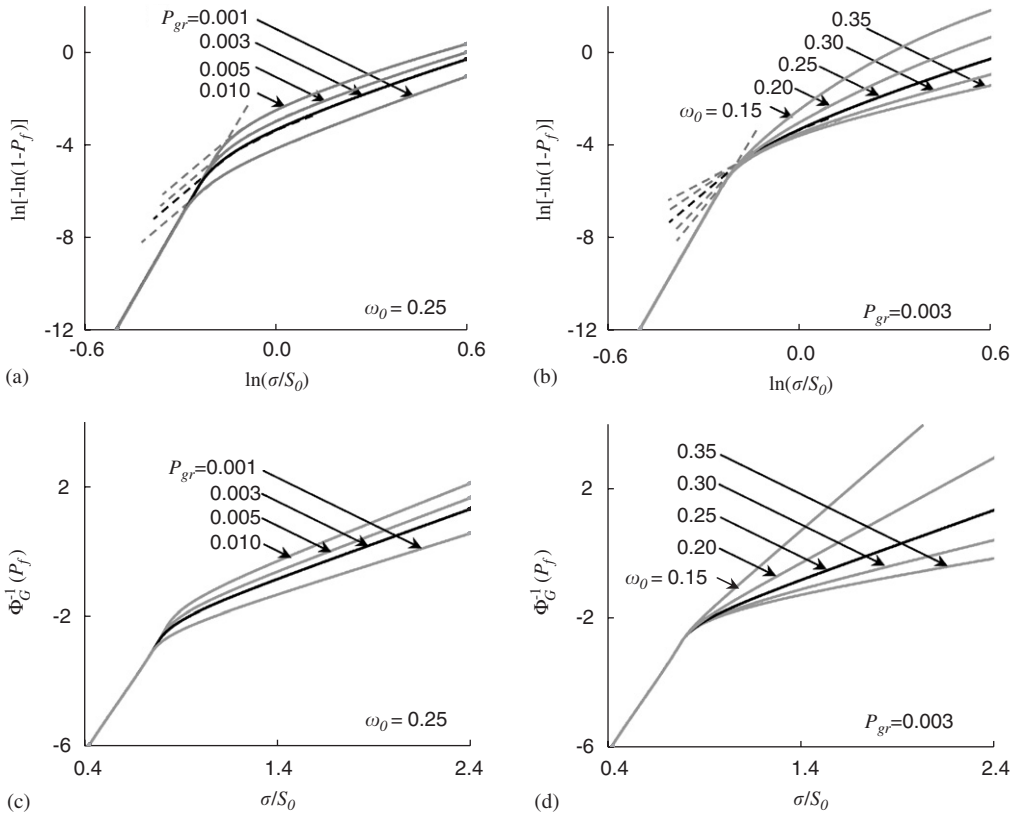


Fig. 7. Effect of the probability at grafting point P_{gr} on the cdf of one RVE with CoV $\omega_0 = 0.25$ plotted in (a) Weibull probability paper; (b) normal probability paper; and the effect of ω_0 (= CoV of one RVE) with grafting probability $P_{gr} = 0.003$ plotted in (c) Weibull probability paper; (d) normal probability paper.

standard deviation of tensile strength for small-size specimens roughly equivalent to one RVE. But determination of s_1 requires tests of very large specimens failing in a brittle manner, which are currently lacking, thus making the explicit approach in Eq. (52) futile. Nevertheless, experimental determination of the CoV for small-size specimens can be used to estimate μ_{Gn} of one RVE based on numerical evaluation of the CoV, ω_θ , of the grafted cdf defined in Eqs. (52), as shown in Table 4 for $\Phi_W(\zeta_{gr})$ ranging from 0.001 to 0.01. Alternatively, δ_{Gn} can be estimated (with error < 5%) from the following empirical equation, allowing explicit determination of the cdf in Eq. (52):

$$\delta_{Gn} = \exp\{-3.254 + 11.566\omega_0 - [1000\Phi_W(\zeta_{gr})/(108.8\Phi_W(\zeta_{gr}) + 0.1334)]\omega_0^2\}. \quad (57)$$

The cdf of an RVE has a Weibull tail, which appears as a straight line on the Weibull probability paper (Figs. 7(a) and (b)), and a Gaussian core, which appears as a straight line on the normal (or Gaussian) probability paper (Figs. 7(c) and (d)). Although, in normal testing, the grafted Weibull tail for one RVE is too short to be detectable, it is nevertheless needed to ensure that a Weibull cdf prevail for large enough quasi-brittle structures, such that $N_{eq} > 300$ to 10,000.

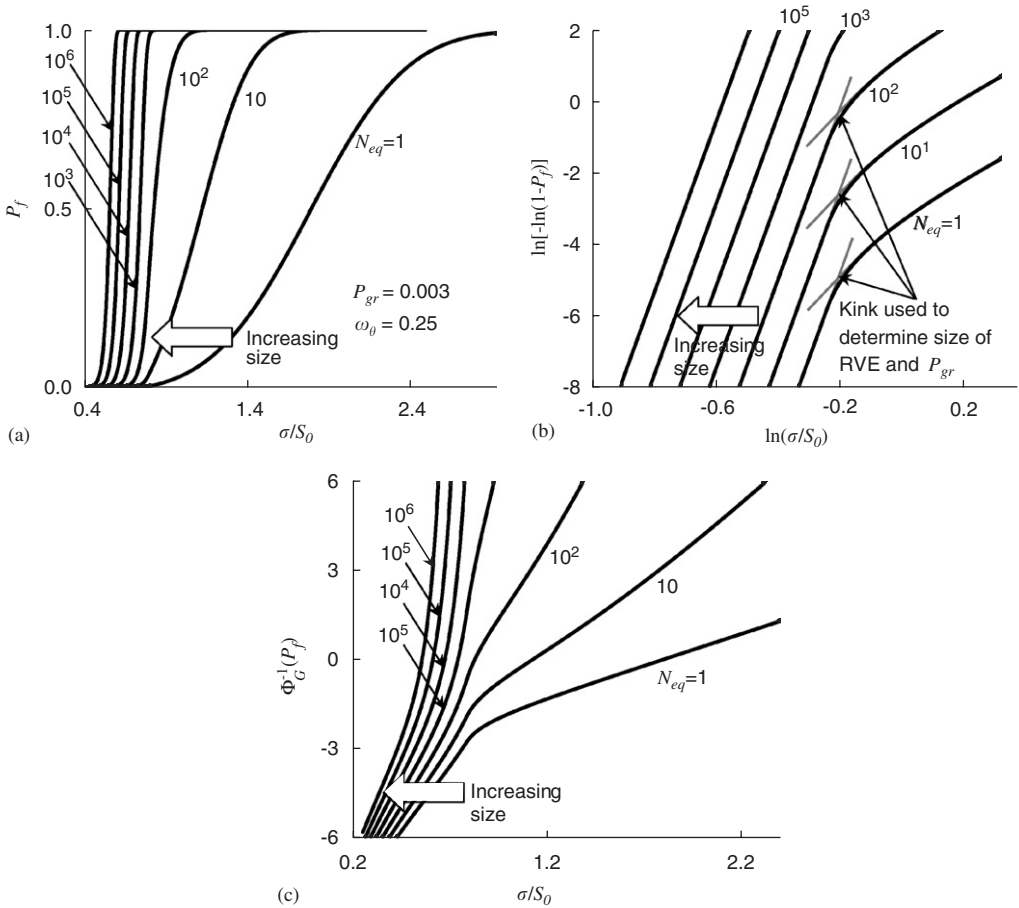


Fig. 8. Size effect on the cdf of structural strength for $P_{gr} = 0.003$, $\omega_0 = 0.25$ in: (a) linear scale (b) Weibull probability paper; (c) normal probability paper.

The cdf of a RVE and the mean size effect depend on four parameters: m , ω_0 , s_1 and P_{gr} . The CoV of one RVE, ω_0 , governs the small-size mean behavior and the slope of the Gaussian core on a normal probability paper (Figs. 7(c) and (d)). The Weibull modulus, m , dictates the Weibull mean size effect for large structure sizes and the slope of Weibull tail on a Weibull probability paper (Figs. 7(a) and (b)), while s_1 scales the nominal strength of the structure and its variation is manifested as a horizontal displacement of the cdf in the normal probability paper. The grafting point probability P_{gr} (i.e., the probability at which the Weibull pdf tail is grafted) controls the structure size at which the full Weibull cdf and the Weibull power-law size effect are attained (Fig. 8(b)). Knowing these four parameters allows determination of all the other statistical properties of one RVE using Eqs. (55)–(57).

The plots in Weibull probability paper in Figs. 7(a) and (b) show the cdf of one RVE for different grafting probabilities P_{gr} , and for different CoVs of the combined cdf.

10. Grafted Weibull–Gaussian cdf for structures equivalent to many RVEs

Since one RVE is defined as a material volume whose failure causes the whole structure to fail, quasibrittle structures that consist of more than one RVE (and have positive geometry, no notches producing stress singularity and no pre-existing large cracks) behave as a chain of RVEs (Fig. 4(f)). The chain survives if and only if all the RVEs survive, $1 - P_f = (1 - P_1)^{N_{eq}}$, and so the failure probability P_f for nominal stress σ_N , which is a common parameter for all the RVEs, is exactly

$$P_f(\sigma_N) = 1 - [1 - P_1(\sigma_N)]^{N_{eq}}, \tag{58}$$

where $P_1(\sigma)$ is the grafted distribution for one RVE. A large enough structure fails at small enough, σ_N , and so the cdf of each RVE must be within the power-law tail, $P_1(\sigma_N) = (\sigma_N/s_0)^m$ (Theorem 1). From Eq. (58) and the well-known limit $\lim_{N \rightarrow \infty} (1 + x/N)^N = e^x$, it follows that

$$P_f(\sigma_N) \approx 1 - \left[1 - \frac{N_{eq}(\sigma_N/s_0)^m}{N_{eq}} \right]^{N_{eq}} \xrightarrow{N_{eq} \rightarrow \infty} 1 - e^{-N_{eq}(\sigma_N/s_0)^m} \tag{59}$$

i.e., the distribution in Eq. (58) becomes Weibull distribution for a structure with a large enough equivalent number of RVEs.

The transition from Gaussian to Weibull cdf when passing from small to large sizes is evident in Fig. 8. On a linear scale of σ_N and P_f (Fig. 8(a)), in which the CoV is proportional to the maximum slope of the cdf curve, the CoV first decreases with increasing N_{eq} , which is typical of bundle (parallel-coupling) statistics, and then stabilizes at a constant value, which is typical of chain (weakest-link) statistics. For $N_{eq} > 1000$ and grafting probability $P_{gr} = 0.001$ of one RVE, the cdf is visually indistinguishable from Weibull cdf and an increase in size causes merely a leftward shift of the cdf curve as a rigid body.

On the Weibull scale (i.e., Weibull probability paper), on which the Weibull cdf of σ_N is a straight line, the straight segment lengthens with increasing N_{eq} (Fig. 8(b)) while the Gaussian core, appearing as a concave curve, shifts upwards. The transition shows up on the histogram as a distinctive kink (Fig. 8(b)), the location of which may be precisely defined as the point of intersection of the extensions of the Gaussian core and the Weibull tail.

On the normal probability paper, on which the Gaussian (normal) cdf of σ_N appears as a straight line, the straight segment shortens with increasing N_{eq} (Fig. 8(c)), while the tail segment of Weibull cdf appears as a curve, shifting and changing shape with N_{eq} .

The mean nominal strength (Fig. 9) for any number of RVEs can be determined as follows:

$$\bar{\sigma}_N = \int_0^\infty \sigma_N N_{eq} [1 - P_1(\sigma_N)]^{N_{eq}-1} p_1(\sigma_N) d\sigma_N. \tag{60}$$

Analytical evaluation of Eq. (60), with $p_1(\sigma_N)$ and $P_1(\sigma_N)$ defined in Eqs. (50)–(51) and (52), respectively, is impossible but the asymptotes can be determined. For large size, the asymptote must be the Weibull size effect, due to the power-law tail of the cdf of each RVE (Hypotheses I and II), which is given by the following expression on a logarithmic scale:

$$\log(\bar{\sigma}_{N,W}) = -(1/m) \log(N_{eq}) + \log[s_0 \Gamma(1 + 1/m)]. \tag{61}$$

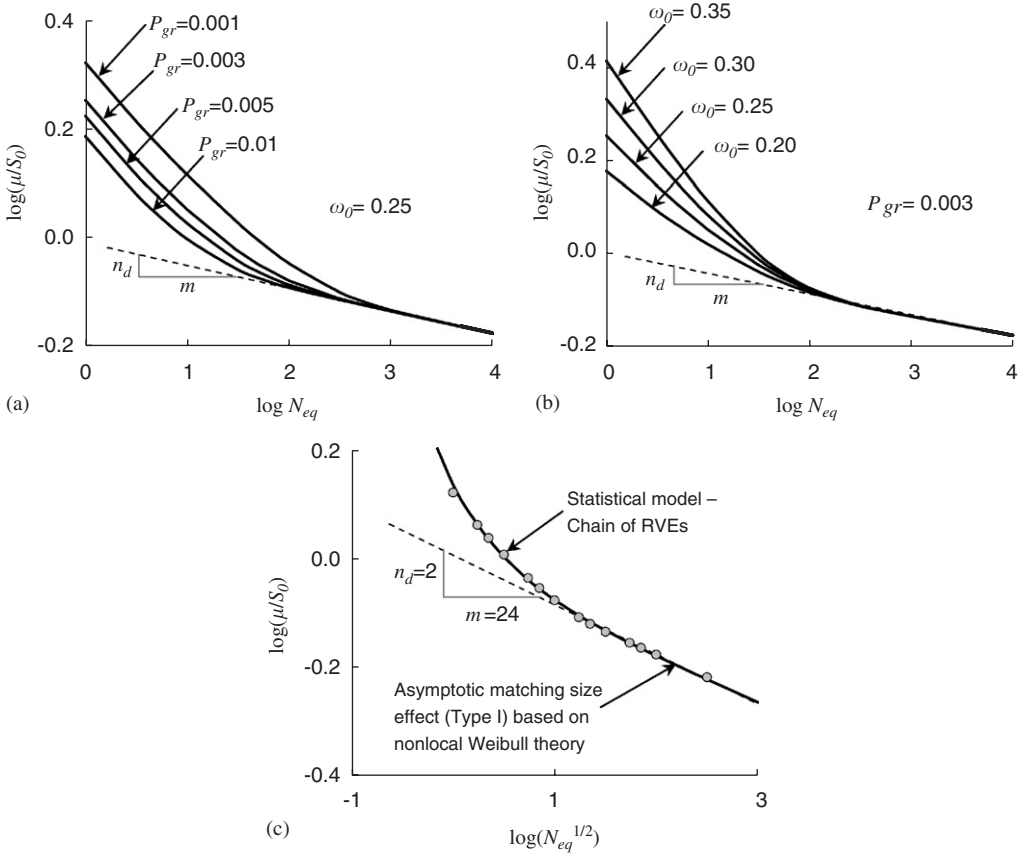


Fig. 9. Size effect on mean nominal strength: (a) for different grafting probability P_{gr} ; or (b) for different CoV of one RVE ω_0 ; and (c) optimum fit of chain-of-RVEs model by the Type 1 size effect law previously obtained by asymptotic matching.

For small sizes (approximately for $N_{eq} \leq 10$), the cdf is predominantly Gaussian and the mean nominal strength for a chain of Gaussian elements may then be calculated as follows:

$$\bar{\sigma}_{N,G} = \int_{-\infty}^{\infty} \frac{\sigma_N N_{eq}}{\delta_G \sqrt{2\pi}} e^{-(\sigma_N - \sigma_G)^2 / 2\delta_G^2} \left[1 - \int_{-\infty}^{\sigma_N} \frac{1}{\delta_G \sqrt{2\pi}} e^{-(\sigma_N - \sigma_G)^2 / 2\delta_G^2} d\sigma'_N \right]^{N_{eq}-1} d\sigma_N. \tag{62}$$

Note that if the tail of all elements were Gaussian rather than a power-law, then, according to the stability postulate (Eq. 23), a long chain would asymptotically approach not the Weibull but the Gumbel distribution. For a Gaussian cdf with an extremely remote power-law tail, and for not too large N_{eq} , the minimum elemental strength in the chain would more likely occur in the Gaussian core rather than the power-law tail, and then the cdf would first appear to approach with increasing N_{eq} the Gumbel distribution, but for large enough N_{eq} it would eventually switch to converging to the Weibull distribution. If such a chain were short, the deviation from Gumbel distribution would still be significant

and the mean nominal strength would then be expressed as

$$\log(\bar{\sigma}_{N,G}) = \mu_G [1 - \chi(N_{\text{eq}})(\omega_0/\sqrt{\pi})], \quad (63)$$

where $\chi(N_{\text{eq}}) = 1, \frac{3}{2}$ for $N_{\text{eq}} = 2, 3$, respectively. For intermediate values, $3 < N_{\text{eq}} < 10$, an analytical expression for parameter μ_s is unavailable (Ang and Tang, 1984). Since even very remote Weibull tails of RVEs spoil approach to Gumbel distribution, even for small N_{eq} , it is necessary that the mean size effect curve in Eq. (60) be obtained by nonlinear regression.

When the asymptotic Weibull strength of Eq. (61) is subtracted from the mean nominal strength (Eq. 60) in logarithmic scale, the difference fits very well the following empirical function:

$$\log(\bar{\sigma}_N) - \log(\bar{\sigma}_{N,W}) = \exp[-\exp(a_1 - a_2 \log(N_{\text{eq}}))], \quad (64)$$

where

$$a_1 = \ln \left[-\ln \left(\log \frac{\mu_0}{s_0 \Gamma(1 + 1/m)} \right) \right]. \quad (65)$$

Parameter a_1 anchors the size effect curve for one RVE; μ_0 is the mean for one RVE; and a_2 controls the rate of transition to Weibull size effect and depends on the length of the Weibull tail for one RVE. Calibrating the mean size effect curve requires identifying at least four parameters: μ_0 , P_{gr} , m , and s_0 .

11. Equivalence to nonlocal Weibull theory

Fig. 9(c) demonstrates another interesting point: The four parameters for the mean size effect, i.e., μ_0 , P_{gr} , m , and s_0 , can be optimized to match very accurately the mean Type 1 energetic-statistical size effect law in Eq. (25) for nonlocal theory, obtained by asymptotic matching (Bažant, 2004a, b). This law, in turn, was further shown to match closely the Monte Carlo simulations with the nonlocal Weibull theory (Bažant and Novák, 2000a, b; Bažant, 2002). This match shows that, on the continuum scale, both theories are equivalent.

It would make no sense to use the present discrete model for structure sizes smaller than one RVE. However, the nonlocal Weibull theory, being a continuum theory, can be extended to structure size $D \rightarrow 0$. Although such extension is a mathematical abstraction of no real physical meaning, it has nevertheless been shown mathematically useful. The mean zero-size asymptotic behavior can be easily determined by considering the FPZ to be perfectly plastic, while the large size asymptotics follows from equivalent LEFM or the smeared-tip model (Bažant, 2002), in which the FPZ shrinks to a point. Thus, the continuum theory makes it possible to obtain mean analytical approximation for any D via asymptotic matching (Bažant, 2004a, b) of the power series expansions, for $D \rightarrow 0$ in terms of powers of D , and for $\rightarrow \infty$ in terms of powers of $1/D$. Derivation of the Type 1 size effect law in Eq. (25) (Bažant, 1997, 2002) is an example.

The mean size effect behavior of the nonlocal Weibull theory is known to be well captured by the cohesive crack model, crack band model or some of the nonlocal damage models for concrete and other quasibrittle materials (Bažant, 2002; Bažant and Planas, 1998). For $D \rightarrow 0$, these models predict a linear approach in terms of D to a finite

‘zero-size’ nominal strength of structure. On a larger scale, all these models should approximately match the mean strength predictions of the present discrete theory.

Consequently, the present theory provides another, statistical, explanation and justification of nonlocal concepts for materials with softening damage or cohesive fracture. In the nonlocal Weibull theory, however, the cdf of strength of the nonlocal averaging volume cannot be predicted and must be assumed. On the basis of the present theory, it may be assumed as the Gaussian cdf with a grafted power-law tail.

12. Verification and calibration

One way to calibrate the present theory is to observe the kink point locations on the experimental histograms of strength of specimens with two sufficiently different $N_{\text{eq}} = N_{\text{eq}1}$ and $N_{\text{eq}2}$, corresponding to sufficiently different specimen sizes $D = D_1$ and D_2 , and possibly to different geometries characterized by $\Psi = \Psi_1$ and Ψ_2 . The specimens must not be too large, so that the kinks are clearly detectable on the histograms. Plotting the histogram on both Weibull and normal probability papers, one can then obtain the Weibull and Gaussian segments of cdf by linear regression of the straight segments of the histograms on each of these two papers. Each histogram may be approximated by a cdf consisting of two semi-infinite segments, Weibull on the left and Gaussian on the right. These segments intersect at a precise kink point, labelled as (σ_{N_i}, P_{f_i}) where $i = 1, 2, \dots$ (Fig. 8(b)). The failure probability at each kink point must be equal to the joint survival probability of all the RVEs subjected to the same σ_N ; this yields:

$$1 - P_{f_i} = [1 - P_1(\sigma_{N_i})]^{N_{\text{eq}_i}}, \quad N_{\text{eq}_i} = (D_i/l_0)\Psi_i \quad (i = 1, 2). \quad (66)$$

Because the stress at each kink point, and thus in each RVE, must be small enough to lie in the power-law tail of cdf of one RVE, we also have $P_1(\sigma_{N_i}) = r_f(\sigma_{N_i}/s_1)^m$ ($i = 1, 2$) where r_f is a known value, $r_f \approx 1$. Substituting this expression into the foregoing equation, one gets two equations from which l_0 can be eliminated. Thus one obtains, after rearrangements:

$$\frac{\ln(1 - P_{f_1})}{\ln(1 - P_{f_2})} = \frac{D_1\Psi_1 \ln[1 - (\sigma_{N_1}/s_0)^m]}{D_2\Psi_2 \ln[1 - (\sigma_{N_2}/s_0)^m]}, \quad (67)$$

where $s_0 = r_f^{1/m} s_1 \approx s_1$. This is a nonlinear equation, from which s_1 can be solved by Newton iterations, and l_0 may then be easily solved from Eq. (66).

Alternatively, one may eliminate s_0 , and this yields for l_0 the nonlinear equation:

$$\frac{1 - (1 - P_{f_1})^{l_0/D_1\Psi_1}}{1 - (1 - P_{f_2})^{l_0/D_2\Psi_2}} = \left(\frac{\sigma_{N_1}}{\sigma_{N_2}}\right)^m \quad (68)$$

from which l_0 can be solved by Newton iterations; s_0 may then be easily solved from Eq. (66).

The grafting point probability for one RVE is then obtained as

$$P_{\text{gr}} = (\sigma_{N_i}/s_0)^m = r_f(\sigma_{N_i}/s_1)^m \quad (i = 1 \text{ or } 2). \quad (69)$$

According to experience with nonlocal models, the size l_0 of one RVE can be roughly estimated as the double or triple of the maximum size of material inhomogeneities. Then it is sufficient to calibrate the model from an experimental strength histogram for one size only ($i = 1$).

If the histogram is measured for more than two sizes D , the values of s_0 and l_0 obtained from any pair of two sizes will not be the same, because of random errors of measurement. Of course, if the values of s_0 and l_0 obtained from different pairs were grossly different, it would disprove the present theory. On the other hand, if they are not too different, it will corroborate the theory.

If histograms for more than two sizes are available, s_0 and l_0 may be obtained by nonlinear least-square optimal fitting of the equation system (68) written for all the sizes tested, $i = 1, 2, \dots, n_t$. In this general case, the use of a nonlinear optimization algorithm such as Marquardt–Levenberg automatically yields the estimates of standard deviations of s_0 and l_0 .

Another way to calibrate the present theory is to fit Eq. (66) to a measured mean size effect curve. This curve must include the smallest specimens that can be fabricated and also specimens so large that Weibull size effect dominates. This way is doubtless more accurate because the scatter of the mean is generally much smaller than the scatter of individual measurements.

Even better results may be obtained by measuring both the histograms and the mean strength for different sizes, and optimally fitting all these results simultaneously with the Levenberg–Marquardt algorithm.

13. Quasi-brittleness or non-zero threshold

For highly homogeneous brittle materials such as fine-grained ceramics, experience shows that their strength histograms can be perfectly fitted by the two-parameter Weibull cdf in Eq. (10), for which the strength threshold vanishes (Weibull, 1939; Bansal et al., 1976a, b; Ito et al., 1981; Katayama and Hattori, 1982; Matsusue et al., 1982; Soma et al., 1985; Brühner-Foit and Munz, 1989; Katz et al., 1993; Lu et al., 2002b). However, for heterogeneous brittle materials, such as concrete, or coarse-grained or transformation-toughened ceramics, the Weibull cdf with zero threshold has been found insufficient, and it has generally been believed that one must use a three-parameter Weibull cdf, having a

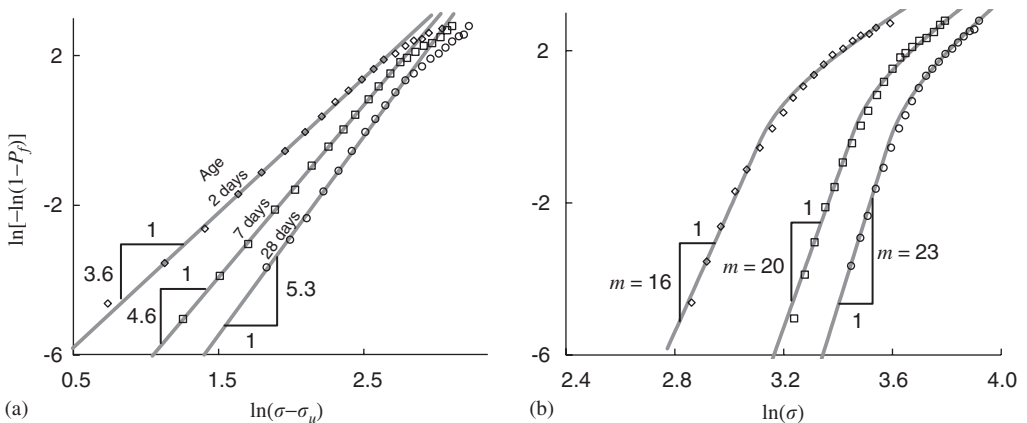


Fig. 10. Optimum fits of Weibull (1939) tests of Portland cement mortar by: (a) Weibull cdfs with finite threshold; (b) chain-of-RVEs model (characterized by zero threshold).

nonzero threshold σ_u , i.e.,

$$\Phi_W(\sigma_N) = 1 - e^{-((\sigma_N - \sigma_u)/s_0)^m}. \quad (70)$$

The first indication of insufficiency of the two-parameter Weibull distribution came from Weibull's (1939) extensive tests of direct tensile strength of Portland cement mortar reproduced in Fig. 10, conducted for three different ages: 2, 7, and 28 days. Although complete identification of the present theory from Weibull's tests is impossible (because the specimen sizes and grain sizes have not been reported), one can nevertheless see that these tests, as well as many subsequent tests of coarse-grained ceramics, typically exhibit a kink separating two segments, just like in Fig. 8 already discussed. These two segments cannot be fitted by Weibull cdf with zero threshold. When the threshold is allowed to be nonzero, the long lower segment of the histogram (straight on Weibull probability paper) can be fitted closely, as shown by Weibull (1939); see Fig. 10(a). However, the kink, and deviation of the upper terminal segment from the extension of the straight lower segment, cannot be fitted. It has been inferred that, for some unexplained reason, the Weibull theory cannot be applied to high probabilities of failure of coarse-grained brittle materials. This limitation has not been regarded as serious because high failure probabilities are not of interest for safe design. It should have been concluded, though, that the pure Weibull theory, even with nonzero threshold, is not applicable.

The present theory [Eq. (58) with (50) and (51)] explains this problem. Fig. 10(b) demonstrates that, unlike the three-parameter Weibull distribution, the present theory allows an excellent fit of Weibull's histograms for mortar over the entire range, with both segments and the kink location matched well. This confirms that the slope change at the kink is explained not by a nonzero threshold but by quasibrittleness, i.e., the fact that l_0 , or the size of RVE, is not negligible compared to cross the section dimension of the structure or specimen.

Even though Weibull did not report sufficient data on his tests of histograms of mortar, one can make at least qualitative deductions. He used the German standard sand, probably the same as today in Eurocode, whose maximum grain size is 2 mm. Accordingly, the RVE size was probably between 0.6 and 1.0 cm, and since the tests were conducted in direct tension, the specimens were almost certainly prisms or cylinders of volume between 100 and 3000 cm³. Thus, his specimen most likely contained between 100 and 10,000 RVEs. From the location of the kink point on his histograms (Fig. 10(b)), it thus follows that the power-law tail of one RVE must have extended up to failure probability between 0.0001 and 0.01. This confirms the soundness of Hypothesis III.

The increasing value of slope m seen in Weibull's histograms for the ages of 2, 7 and 28 days can be explained by chemical hardening due to cement hydration. With increasing age, the hardened cement paste binding the grains is getting stiffer and the bond to sand grains stronger, which makes the material more homogeneous. Hence, one must expect a reduction of scatter, which implies an increase of m . The shift of kink up and right (i.e., to larger strength) is explained by increasing RVE strength caused by hardening of the cement paste with age.

Note that the fitting of the present theory to strength histograms of not too large specimens generally yields a higher value of Weibull modulus m than the fitting of three-parameter cdf to the lower segment of the histogram. This matches (and thus reinforces) the earlier finding of Bažant and Novák, (2000a, b), namely that the fitting of size effect data with the nonlocal Weibull theory (Eq. 9(c)), which is a continuum theory, yields a

higher value of m than the estimation of m by pure Weibull theory from the CoV of small specimen strengths, and that only this higher value matches the CoV of strength for large sizes. Based on the CoV of strength tests for small concrete specimens, it used to be believed that, for concrete, $m \approx 12$. But the nonlocal Weibull theory showed that the consistent and correct value is $m \approx 24$ (Bažant and Novák, 2000a, b). The present theory, which is a discrete theory, leads to the same conclusion (see Fig. 10(b)), which is not unexpected.

Quasi-brittleness is a relative concept. With regard to the current emphasis on nano-technology, note that moving toward the micrometer or nanometer scale, every brittle material becomes quasibrittle. Thus, in micromechanics of MEMS, it must be expected that modelling of a ceramic with the grain size of $1 \mu\text{m}$ would require the present chain-of-RVEs model (or nonlocal Weibull theory) when the cross section dimension is $2 \mu\text{m}$ to 0.5 mm . On the other hand, for the ice cover of the Arctic Ocean, in which the grains are represented by ice floes about 3 km in size and 2 to 6 m thick, embedded in a matrix of refrozen water leads about 0.3 m thick, one must expect the present theory to apply for two-dimensional floating ice bodies larger than about 6 km , and the pure Weibull theory for bodies larger than about 1000 km .

A finite threshold strength has recently been reported for laminar ceramics (Rao et al., 1999). But this is not the threshold strength in Weibull context. Rather, these tests involved interlaminar failure of laminar ceramics subjected to tension along the lamina. However, some lamina were preloaded in compression during fabrication and were still in compression at failure, thus engendering an apparent residual strength in the laminar specimen as a whole after some lamina have failed.

14. Tail of distribution of yield strength of plastic materials

In plastic materials, the nucleation and glide of dislocations is also governed, on the atomic scale, by activation energy barriers. So why the yield strength of plastic materials and structures of any size follows a Gaussian rather than Weibull cdf?

The likely reason is twofold: (1) statistical behavior corresponding to parallel coupling of more than about four elements, and (2) lack of softening in the elements of a hierarchical model, allowing many elements to reach their random strength limits almost simultaneously. The statistical sub-bundles that connect nano to macro are very wide, i.e., involve then not just two or three but many elements coupled in parallel. This has been shown to yield an absolutely negligible power-law tail, so short that even a series coupling of many sub-bundles cannot produce a Weibull cdf. Thus, even though the cdf of yield strength of a plastic material must have a power-law tail, this tail is so remote from the mean that it can play no role at all.

15. Remark on nanotubes and other long nano-structures

According to the hierarchical model (Fig. 4(f)), at nanometer scale one may expect much fewer statistically parallel connections. This means that the tail exponent of 1 at atomic scale might not be raised much by parallel couplings, and a left-tail power-law exponent as small as 2 – 6 could be logically expected. Considering two-dimensional scaling of failure ($n_d = 2$), this would imply, for sufficiently long nanostructures, a size effect between D^{-1} and $D^{-1/3}$.

Such a strong statistical size effect (possibly superposed on the gradient and boundary layer size effects; Bažant et al., 2005a; Guo and Bažant, 2004) would greatly weaken very long nanotubes, thin films and other nano-structures. But it could be mitigated by creating parallel couplings, e.g. by creating cross-linking in multiple or parallel nanotubes.

16. Dependence of grafted cdf on temperature and loading rate or duration

The present model also predicts the dependence of the grafted distribution on T and τ . This offers another possibility to verify the model experimentally.

The dependence on T and τ is simple for large enough quasibrittle structures perfectly following the Weibull distribution; namely, the scaling parameter s_0 must depend on T and τ in the same way as indicated in Eq. (6), while the Weibull modulus (shape parameter) and the CoV remain unaffected by T and τ .

Quasibrittle structures, and certainly specimens of quasibrittle materials, will typically not be large enough to have a perfect Weibull distribution. For the grafted cdf, applicable to smaller structural sizes, the dependence on T and τ , which can be figured out from the present model, is more complicated. Not only s_0 but also the mean and CoV of the combined grafted cdf, will be affected. This problem and statistical experiments at various T and τ needed to justify the present theory experimentally are planned for a subsequent study.

17. Conclusions

1. The understrength part of safety factors for quasibrittle structures cannot be constant, as generally assumed today, but must be increased with structure size and changed as a function of structure geometry.
2. The four basic questions raised at the outset are answered:
 - (a) The physical reason why the tail of the cumulative density function (cdf) of strength of RVE of any material (whether brittle or plastic) must be a power law, is that the failure of interatomic bonds is a thermally activated process governed by stress-dependent activation energy barriers. This further implies that the cdf of a brittle or large enough quasibrittle structure must follow Weibull cdf.
 - (b) The threshold of power-law tail and of the Weibull cdf of strength must be zero because, according to Maxwell–Boltzmann distribution of atomic thermal energies, the threshold stress for the net rate of interatomic bond breaks is zero.
 - (c) The physical meaning of Weibull modulus m is the number of dominant bonds that must be severed, or the number of matrix connections between adjacent major inhomogeneities that must fail, in order to cause failure of the representative volume of material (RVE). This number must in some way depend on the spatial packing of inhomogeneities in the RVE.
 - (d) The reason why the exponent of the power-law tail (and the Weibull modulus) is so high (ranging from 10 to 50), is that every parallel statistical coupling of bonds within a RVE raises the exponent, beginning with the exponent of 1 at the atomic scale.
3. The multiplier (or amplitude) of the power-law tail of the cdf of strength of quasibrittle structures is the same function of absolute temperature T and load duration τ as that

indicated by Maxwell–Boltzmann distribution for the rate of breaks of interatomic bonds.

4. The statistical model for RVE can include parallel connections of no more than two elements on scales close to macroscales (with power-law tail exponent greater than about 6), and three elements on lower scales (with power-law tail exponent less than about 6), or else the power-law tail of cdf of RVE strength would be so short that Weibull distribution would never be observed in practice.
5. While the power-law tail exponent of a chain is equal to the lowest exponent among its links, the power-law tail exponent of a bundle is equal to the sum of the power-law tail exponents of all the parallel fibers in a bundle, regardless of whether they are brittle or plastic (the same is probably true for softening fibers). While the extent of power-law tail increases with the length of a chain, it drastically decreases (in cdf scale) with the number of fibers in a bundle.
6. A sufficiently long power-law tail of RVE strength can be reconciled with the activation energy concept only if the RVE is statistically modelled by a hierarchy of parallel and series couplings, consisting of bundles of sub-chains of sub-bundles of sub-sub-chains of sub-sub-bundles, etc., down to the atomic scale. The Weibull modulus is equal to the minimum number of cuts of elementary bonds needed to separate the hierarchical model into two parts. The elements of the sub-chains and sub-bundles in the hierarchical model may exhibit plastic or softening behaviors, but not a perfectly brittle behavior because such behavior would not allow a sufficiently long power-law tail of the cdf of RVE. The cdf of RVE strength cannot be modelled by a bundle with a finite number of elements following the Maxwell–Boltzmann distribution, and quasibrittle structures cannot be modelled as a chain of bundles. Otherwise, the power-law tail of RVE would be far too short for generating Weibull cdf for the strength of large structures.
7. For the sake of engineering computations, the cdf of random strength of a RVE may be assumed to have Weibull left tail grafted at the failure probability of about 0.0001–0.01 onto a Gaussian core. With increasing structure size, the grafting point moves to higher failure probabilities as a function of the equivalent number of RVEs, in a way than can be described by treating the structure as a chain of finite RVEs. The mean and CoV of this grafted distribution are easy to calculate and are tabulated.
8. For not too small structures, the present chain-of-RVEs model gives similar results as the previously developed nonlocal Weibull theory, while for very small structures (not much larger than a RVE) it allows predicting failure probability more rationally. The mean behavior is, on not too small scales, essentially equivalent to that of the cohesive crack model, crack band model and nonlocal damage models.
9. The theory explains why a nonzero threshold was found preferable in previous studies of coarse-grained ceramics and concrete. The reason is that the strength histograms of these materials exhibit a kink separating a lower Weibull segment from an upper Gaussian segment. The lower segment up to the kink, important for safe design, can be fitted by Weibull cdf with a finite threshold. But the upper segment cannot. The present theory removes this problem. The predicted cdf fits both segments of the experimental histograms, along with the kink location, very well. This is one experimental verification of the present theory.
10. Two ways of experimental calibration and verification are proposed. (1) Fit the mean size effect curve, particularly its deviation from the Weibull size effect for small sizes.

(2) Fit the strength histograms with kinks for at least two significantly different sizes (and possibly different shapes). Each way suffices to determine all the parameters. Still another check is fitting of experimental strength histograms for different temperatures, loading rates or load durations.

Acknowledgments

Partial financial support under ONR Grant N00014-10-I-0622 and NSF Grant CMS-0556323 (both to Northwestern University), and a Grant from Infrastructure Technology Institute at Northwestern University, is gratefully acknowledged. Thanks for stimulating discussions are due to Martin Z. Bazant, Associate Professor of Mathematics at M.I.T., to Drahomír Novák, Professor at VUT Brno, and to Miroslav Vořechovský, Assistant Professor at VUT Brno, Czech Republic.

References

- Amar, E., Gauthier, G., Lamon, J., 1989. Reliability analysis of a Si_3N_4 ceramic piston pin for automotive engines. In: Tennery, V. (Ed.), *Ceramics Materials and Components for Engines*. American Ceramic Society, Westerville, OH, pp. 1334–1346.
- Ang, A.H.-S., Tang, W.H., 1984. *Probability Concepts in Engineering Planning and Design*. vol. II. Decision, Risk and Reliability. Wiley, New York.
- Bansal, G.K., Duckworth, W.H., Niesz, D.E., 1976a. Strength-size relations in ceramic materials: Investigation of an alumina ceramic. *J. Am. Ceram. Soc.* 59, 472–478.
- Bansal, G.K., Duckworth, W.H., Niesz, D.E., 1976b. Strength analysis of brittle materials. Battelle-Report, Columbus.
- Bartlett, F.M., MacGregor, J.G., 1996. Statistical analysis of the compressive strength of concrete in structures. *ACI Mat. J.* 93 (2), 158–168.
- Bažant, Z.P., 1984. Size effect in blunt fracture: concrete, rock, metal. *J. Eng. Mech. ASCE* 110 (4), 518–535.
- Bažant, Z.P., 1995. Creep and damage in concrete. In: Skalny, J., Mindess, S. (Eds.), *Materials Science of Concrete IV*. American Ceramic Society, Westerville, OH, pp. 355–389.
- Bažant, Z.P., 1997. Scaling of quasibrittle fracture: Asymptotic analysis. *Int. J. Fract.* 83 (1), 19–40.
- Bažant, Z.P., 2002. *Scaling of Structural Strength* (second ed.), Hermes Penton Science (Kogan Page Science), London, U.K Elsevier, London 2005; French translation, Hermès, Paris 2004.
- Bažant, Z.P., 2004a. Probabilistic distribution of energetic-statistical size effect in quasibrittle fracture. *Probabilistic Eng. Mech.* 19 (4), 307–319.
- Bažant, Z.P., 2004b. Scaling theory for quasibrittle structural failure. *Proc. Nat. Acad. Sci.* 101 (37), 13397–13399.
- Bažant, Z.P., Jirásek, M., 1993. R-curve modeling of rate and size effects in quasibrittle fracture. *Int. J. Fract.* 62, 355–373.
- Bažant, Z.P., Li, Y.-N., 1997. Cohesive crack with rate-dependent opening and viscoelasticity: I. Mathematical model and scaling. *Int. J. Fract.* 86 (3), 247–265.
- Bažant, Z.P., Novák, D., 2000a. Probabilistic nonlocal theory for quasibrittle fracture initiation and size effect. II. Application. *J. Eng. Mech. ASCE* 126 (2), 175–185.
- Bažant, Z.P., Novák, D., 2000b. Energetic-statistical size effect in quasibrittle failure at crack initiation. *ACI Mater. J.* 97 (3), 381–392.
- Bažant, Z.P., Novák, D., 2001. Nonlocal model for size effect in quasibrittle failure based on extreme value statistics. In: Corotis, R.B. (Ed.), *Proceedings of the Eighth International Conference on Structural Safety and Reliability (ICOSSAR)*, Newport Beach, CA., 2001, Swets & Zeitinger, Balkema, pp. 1–8.
- Bažant, Z.P., Pang, S.D., 2005a. Revision of reliability concepts for quasibrittle structures and size effect on probability distribution of structural strength. In: Augusti, G., Schuëller, G.I., Ciampoli, M., (Eds.), *Proceedings of Ninth International Conference on Structural Safety and Reliability (ICOSSAR)*, Rome, Milpress, Rotterdam, pp. 377–386.

- Bažant, Z.P., Pang, S.-D., 2005b. Effect of size on safety factors and strength of quasibrittle structures: Beckoning reform of reliability concepts. In: Chandra Kishen, J.M., Roy, D. (Eds.), *Proceedings of the Structural Engineering Convention (SEC 2005)*. Indian Institute of Science, Bangalore, India, pp. 2–20.
- Bažant, Z.P., Pang, S.-D., 2006. Mechanics based statistics of failure risk of quasibrittle structures and size effect on safety factors. *Proceedings of the National Academy of Sciences*, vol. 103(25), 9434–9439.
- Bažant, Z.P., Planas, J., 1998. *Fracture and Size Effect in Concrete and Other Quasibrittle Materials*. CRC Press, Boca Raton, FL.
- Bažant, Z.P., Prat, P.C., 1988. Effect of temperature and humidity on fracture energy of concrete. *ACI Mater. J.* 84, 262–271.
- Bažant, Z.P., Xi, Y., 1991. Statistical size effect in quasi-brittle structures: II. Nonlocal theory. *J. Eng. Mech. ASCE* 117 (17), 2623–2640.
- Bažant, Z.P., Yu, Q., 2006. Reliability, brittleness and fringe formulas in concrete design codes. *J. Struct. Eng. ASCE* 132(1), 3–12.
- Bažant, Z.P., Gu, W.-H., Faber, K.T., 1995. Softening reversal and other effects of a change in loading rate on fracture of concrete. *ACI Mater. J.* 92, 3–9.
- Bažant, Z.P., Guo, Z., Espinosa, H., Zhu, Y., Peng, B., 2005. Epitaxially influenced boundary layer model for size effect in thin metallic films. *J. Appl. Phys.* 97, 073506-1–073506-13.
- Bažant, Z.P., Vořechovský, M., Novák, M., 2005b. Asymptotic prediction of energetic-statistical size effect from deterministic finite element solutions. *J. Eng. Mech. ASCE*, in press.
- Beremin, F.M., 1983. A local criterion for cleavage fracture of a nuclear pressure vessel steel. *Metall. Trans.* 114A, 2277–2287.
- Bouchaud, J.-P., Potters, M., 2000. *Theory of Financial Risks: From Statistical Physics to Risk Management*. Cambridge University Press, Cambridge, UK.
- Breyse, D., 1990. A probabilistic formulation of the damage evaluation law. *Struct. Saf.* 8, 311–325.
- Brühner-Foit, A., Munz, D., 1989. Statistical analysis of flexure strength data. *Int. Energy Agency Annex II*, Subtask 4.
- Bulmer, M.G., 1967. *Principles of Statistics*. Dover, New York.
- Carmeliet, J., 1994. In: Kusters, G.M.A., Hendriks, M.A.N. (Eds.), *On Stochastic Descriptions for Damage Evolution in Quasi-Brittle Materials*. DIANA Computational Mechanics.
- Carmeliet, J., Hens, H., 1994. Probabilistic nonlocal damage model for continua with random field properties. *J. Eng. Mech. ASCE* 120, 2013–2027.
- Chmielewski, T., Konopka, E., 1999. Statistical evaluations of field concrete strength. *Mag. Concr. Res.* 51 (1), 45–52.
- CIRIA, 1977. *Rationalization of safety and serviceability factors in structural codes*. Construction Industry Research and Information Association, Report no. 63. London.
- Cornell, C.A., 1969. A probability based structural code. *ACI J.* 66 (12), 974–985.
- Cottrell, A.H., 1964. *The Mechanical Properties of Matter*. Wiley, New York.
- Curtin, W.A., Scher, H., 1997. Time-dependent damage evolution and failure in materials. I. Theory. *Phys. Rev. B* 55 (18), 12038–12050.
- Cusatis, G., Bažant, Z.P., Cedolin, L., 2003. Confinement-shear lattice model for concrete damage in tension and compression: I. Theory. *J. Eng. Mech. ASCE* 129 (12), 1439–1448.
- Daniels, H.E., 1945. The statistical theory of the strength of bundles and threads. *Proc. R. Soc. London A* 183, 405–435.
- Danzer, R., Lube, T., 1996. New fracture statistics for brittle materials. *Fract. Mech. Ceram.* 11, 425–439.
- Duckett, W., 2005. Risk analysis and the acceptable probability of failure. *The Struct. Eng.* 83 (15), 25–26.
- Ellingwood, B.R., McGregor, J.G., Galambos, T.V., Cornell, C.A., 1982. Probability based load criteria: load factors and load combinations. *J. Struct. Eng. ASCE* 108 (ST5), 978–997.
- Erntroy, H.C., 1960. *The variation of works test cubes*. Slough, Cement and Concrete Association, Research Report 10. Publication 41.010, Slough, UK.
- Eyring, H., 1936. Viscosity, plasticity and diffusion as examples of absolute reaction rates. *J. Chem. Phys.* 4, 263.
- Eyring, H., Lin, S.H., Lin, S.M., 1980. *Basic Chemical Kinetics*. Wiley, New York.
- Feller, W., 1957. *Introduction to Probability Theory and its Applications*, second ed. Wiley, New York.
- FHWA (Federal Highway Administration) 1998. *Concrete strength. Guide to Developing Performance-Related Specifications for PCC Pavement—Technical Summary*. vol. 3, App. C.
- Fisher, R.A., Tippett, L.H.C., 1928. Limiting forms of the frequency distribution of the largest and smallest member of a sample. *Proc. Cambridge Philos. Soc.* 24, 180–190.

- Frantziskonis, G.N., 1998. Stochastic modeling of heterogeneous materials—A process for the analysis and evaluation of alternative formulations. *Mech. Mater.* 27, 165–175.
- Fréchet, M., 1927. Sur la loi de probabilité de l'écart maximum. *Ann. Soc. Pol. Math.* 6, 93–116.
- Freudenthal, A.M., 1968. Statistical approach to brittle fracture. In: Liebowitz, H. (Ed.), *Fracture: An Advanced Treatise*, vol. 2. Academic Press, New York, pp. 591–619.
- Freudenthal, A.M., Garrelts, J.M., Shinozuka, M., 1966. The analysis of structural safety. *J. Struct. Div. ASCE* 92 (ST1), 619–677.
- Gehrke, E., Liebelt, A., Hollstein, T., 1993. Der Zugversuch—Technischer Stand und Perspektive. In: *Mechanische Eigenschaften keramischer Konstruktionswerkstoffe*. DGM Informationsgesellschaft, pp. 291–306.
- Glasstone, S., Laidler, K.J., Eyring, H., 1941. *The Theory of Rate Processes*. McGraw-Hill, New York.
- Gumbel, E.J., 1958. *Statistics of Extremes*. Columbia University Press, New York.
- Guo, Z., Bažant, Z.P., 2004. Theoretical modeling and scaling. Section 4, pp. 584–592, 596–600. In: B.C. Prorok, Y. Zhu, H.D. Espinosa, Z. Guo, Z.P. Bažant, Y. Zhao, B.I. Yakobson (Eds.), *Micro- and Nanomechanics*, vol. 5, pp. 555–600. In: H.S. Nalva (Ed.), *Encyclopedia of Nanoscience and Nanotechnology*, American Scientific Publishers, Stevenson Ranch, CA.
- Gutiérrez, M.A., 1999. Objective simulation of failure in heterogeneous softening solids. Dissertation, Delft University of Technology.
- Haldar, A., Mahadevan, S., 2000. *Probability, Reliability and Statistical Methods in Engineering Design*. Wiley, New York.
- Harlow, D.G., Phoenix, S.L., 1978a. The chain-of-bundles probability model for the strength of fibrous materials. I. Analysis and conjectures. *J. Compos. Mater.* 12, 195–214.
- Harlow, D.G., Phoenix, S.L., 1978b. The chain-of-bundles probability model for the strength of fibrous materials. II: A numerical study of convergence. *J. Compos. Mater.* 12, 314–334.
- Harlow, D.G., Smith, R.L., Taylor, H.M., 1983. Lower tail analysis of the distribution of the strength of load-sharing systems. *J. Appl. Probab.* 20, 358–367.
- Hattori, Y., Tajima, Y., Yabuta, K., Matsuo, J., Kawamura, M., Watanabe, T., 1989. Gas pressure sintered silicon nitride ceramics for turbocharger applications. In: Tennery, V. (Ed.), *Ceramics Materials and Components for Engines*. American Ceramic Society, Westerville, OH, pp. 166–172.
- Hill, T.L., 1960. *An Introduction to Statistical Mechanics*. Addison-Wesley, Reading, MA.
- Ito, S., Sakai, S., Ito, M., 1981. Bending strength of hot-pressed silicon nitride. *Zairyo* 30 (337), 1019–1024.
- Jackson, K.E., 1992. Scaling effects in the flexural response and failure of composite beams. *AIAA J.* 30 (8), 2099–2105.
- Julian, O.G., 1955. Discussion of “Strength variations in ready-mixed concrete” by A.E. Cummings. *ACI Proc.* 51 (12), 772–778.
- Katayama, Y., Hattori, Y., 1982. Effects of specimen size on strength of sintered silicon nitride. *J. Am. Ceram. Soc.* 65(10), C-164–C-165.
- Katz, R.N., Wechsler, G., Toutjanjim, H., Friel, D., Leatherman, G.L., El-Korchi, T., Rafaniello, W., 1993. Room temperature tensile strength of AlN. *Ceram. Eng. Sci. Proc.* 14, 282–291.
- Koide, H., Akita, H., Tomon, M., 1998. Size effect on flexural resistance due to bending span of concrete beams. In: Mihashi, H., Rokugo, K. (Eds.), *Fracture Mechanics of Concrete Structures*, Proceedings of the Third International Conference on FraMCoS-3 held in Gifu, Japan. Aedificatio Publishers, Freiburg, Germany, pp. 2121–2130.
- Koide, H., Akita, H. and Tomon, M., 2000. Probability model of flexural resistance on different lengths of concrete beams, in: R.E. Melchers, M.G. Stewart, (Eds.), *Application of Statistic and Probability*, Proceedings of the Eighth International Conference, ICASP-8, held in Sydney, Australia, 1999, Balkema, Rotterdam, vol. 2, pp. 1053–1057.
- Lu, C., Danzer, R., Fischer, F.D., 2002a. Fracture statistics of brittle materials: Weibull or normal distribution. *Physical Review E* 65, 067102-1–067102-4.
- Lu, C., Danzer, R., Fischer, F.D., 2002b. Influence of threshold stress on the estimation of the Weibull statistics. *J. Am. Ceram. Soc.* 85 (6), 1640–1642.
- Madsen, H.O., Krenk, S., Lind, N.C., 1986. *Methods of Structural Safety*. Prentice-Hall, Englewood Cliffs, NJ.
- Mahesh, S., Phoenix, S.L., Beyerlein, I.J., 2002. Strength distributions and size effects for 2D and 3D composites with Weibull fibers in an elastic matrix. *Int. J. Fract.* 115, 41–85.
- Matsusue, K., Takahara, K., Hashimoto, R., 1982. Strength evaluation of hot-pressed silicon nitride at room temperature. *Yogyo Kyokai Shi* 90 (4), 168.
- Mayer, J.E., 1940. *Statistical Mechanics*. Wiley, New York.

- McCartney, L.N., Smith, R.L., 1983. Statistical theory of the strength of fiber bundles. *J. Appl. Mech.* 50, 601–608.
- McClintock, A.M., Argon, A.S. (Eds.), 1966. *Mechanical Behavior of Materials*. Addison-Wesley, Reading, MA.
- McMeeking, R.M., Hbaieb, K., 1999. Optimal threshold strength of laminar ceramics. *Z. Metallk.* 90 (12), 1031–1036.
- Melchers, R.E., 1987. *Structural Reliability, Analysis & Prediction*. Wiley, New York.
- Metcalfe, J.B., 1970. The specification of concrete strength. Part II. The distribution of concrete for structures in current practice. Crowthorne, Road Research Laboratory. Report LR 300.
- Mirza, S.A., Hatzinikolas, M., MacGregor, J.G., 1979. Statistical descriptions of strength of concrete. *J. Struct. Div. ASCE* 105 (ST6), 1021–1037.
- Neaman, D., Laguros, J.G., 1967. Statistical quality control in Portland cement concrete pavements, Transportation research record 184, Transportation Research Board, pp. 1–12.
- Newman, W.I., Phoenix, S.L., 2001. Time-dependent fiber bundles with local load sharing. *Phys. Rev. E* 63, 021507-1–012507-20.
- NKB (Nordic Committee for Building Structures) 1978. Recommendation for loading and safety regulations for structural design. NKB Report, no. 36.
- Ohji, T., 1988. Towards routine tensile testing. *Inter. J. High Technol. Ceram.* 4, 211–225.
- Phoenix, S.L., 1978. The asymptotic time to failure of a mechanical system of parallel members. *SIAM J. Appl. Math.* 34 (2), 227–246.
- Phoenix, S.L., 1983. The stochastic strength and fatigue of fiber bundles. *Int. J. Fract.* 14, 327–344.
- Phoenix, S.L., Beyerlein, I.J., 2000. Distribution and size scalings for strength in a one-dimensional random lattice with load redistribution to nearest and next nearest neighbors. *Phys. Rev. E* 62 (2), 1622–1645.
- Phoenix, S.L., Smith, R.L., 1983. A comparison of probabilistic techniques for the strength of fibrous materials under local load-sharing among fibers. *Int. J. Solids Struct.* 19 (6), 479–496.
- Phoenix, S.L., Tierney, L.-J., 1983. A statistical model for the time dependent failure of unidirectional composite materials under local elastic load-sharing among fibers. *Eng. Fract. Mech.* 18 (1), 193–215.
- Phoenix, S.L., Ibnabdeljalil, M., Hui, C.-Y., 1997. Size effects in the distribution for strength of brittle matrix fibrous composites. *Int. J. Solids Struct.* 34 (5), 545–568.
- Quinn, G.D., 1990. Flexure strength of advanced structural ceramics, a round robin. *J. Am. Ceram. Soc.* 73 (8), 2374–2384.
- Quinn, G.D., Morrell, R., 1991. Design data for engineering ceramics: a review of the flexure test. *J. Am. Ceram. Soc.* 74 (9), 2037–2066.
- Rao, M.P., Sánchez-Herencia, A.J., Beltz, G.E., McMeeking, R.M., Lange, F.F., 1999. Laminar ceramics that exhibit a threshold strength. *Science* 286, 102–104.
- Rüsch, H., Sell, R., Rackwitz, R., 1969. Statistical analysis of concrete strength. *Deutscher Ausschuss Stahlbeton Heft* 206.
- Santos, C., Strecker, K., Neto, F.P., Silva, O.M.M., Baldacim, S.A., Silva, C.R.M., 2003. Evaluation of the reliability of $\text{Si}_3\text{N}_4\text{-Al}_2\text{O}_3\text{-CTR}_2\text{O}_3$ ceramics through Weibull analysis. *Mater. Res.* 6 (4), 463–467.
- Sato, S., Taguchi, K., Adachi, R., Nakatani, M., 1996. A study on strength characteristics of Si_3N_4 coil springs. *Fatigue Fract. Eng. Mater. Struct.* 19 (5), 529–537.
- Shalon, R., Reintz, R.C., 1955. Interpretation of strengths distribution as a factor in quality control of concrete. *Proc. Réunion Int. des Lab. d'Essais et de Recherches sur les Matériaux et les Constr., Symp on the Observation of Sub-struct., vol. 2, Laboratório Nacional de Engenharia Civil, Lisbon, Portugal*, pp. 100–116.
- Smith, R.L., 1982. The asymptotic distribution of the strength of a series-parallel system with equal load sharing. *Ann. Probab.* 10 (1), 137–171.
- Smith, R.L., Phoenix, S.L., 1981. Asymptotic distributions for the failure of fibrous materials under series-parallel structure and equal load-sharing. *J. Appl. Mech.* 48, 75–81.
- Soma, T., Matsui, M., Oda, I., 1985. Tensile strength of a sintered silicon nitride. In: *Proceedings of Non-oxide Technical and Engineering Ceramics, Limerick, Ireland, July 10–12 1985*, pp. 361–374.
- Soong, T.T., 2004. *Fundamentals of Probability and Statistics for Engineers*. Wiley, New York.
- Tobolsky, A.V., 1960. *Structure and Properties of Polymers*. Wiley, New York.
- Weibull, W., 1939. The phenomenon of rupture in solids. *Proceedings of Royal Swedish Institute of Engineering Research* vol. 151, Stockholm, pp. 1–45.
- Weibull, W., 1951. A statistical distribution function of wide applicability. *J. Appl. Mech. ASME* 153 (18), 293–297.
- Zhurkov, S.N., 1965. Kinetic concept of the strength of solids. *Int. J. Fract. Mech.* 1 (4), 311–323.
- Zhurkov, S.N., Korsukov, V.E., 1974. Atomic mechanism of fracture of solid polymers. *J. Polym. Sci.* 12 (2), 385–398.